

# Current State of Fibrotic Interstitial Lung Disease Imaging

Lydia Chelala, MD<sup>1</sup> • Anupama G. Brixey, MD<sup>2,3</sup> • Stephen B. Hobbs, MD<sup>4</sup> • Jeffrey P. Kanne, MD<sup>5</sup> • Seth J. Kligerman, MD<sup>6</sup> • David A. Lynch, MD<sup>6</sup> • Jonathan H. Chung, MD<sup>1,7</sup>

Author affiliations, funding, and conflicts of interest are listed at the end of this article.

See also the editorial by Egashira in this issue.

Radiology 2025; 316(1):e242531 • <https://doi.org/10.1148/radiol.242531> • Content codes: **CH** **CT**

Interstitial lung disease (ILD) diagnosis is complex, continuously evolving, and increasingly reliant on thin-section chest CT. Multidisciplinary discussion aided by a thorough radiologic review can achieve a high-confidence diagnosis of ILD in the majority of patients and is currently the reference standard for ILD diagnosis. CT also allows the early recognition of interstitial lung abnormalities, possibly reflective of unsuspected ILD and progressive in a substantial proportion of patients. Beyond diagnosis, CT has also become essential for ILD prognostication and follow-up, aiding the identification of fibrotic and progressive forms. The presence of fibrosis is a critical determinant of prognosis, particularly when typical features of usual interstitial pneumonia (UIP) are identified. The UIP-centric imaging approach emphasized in this review is justified by the prognostic significance of UIP, the prevalence of UIP in idiopathic pulmonary fibrosis, and its strong radiologic-pathologic correlation. In nonidiopathic pulmonary fibrosis ILD, progressive pulmonary fibrosis carries clinically significant prognostic and therapeutic implications. With growing evidence and the emergence of novel ILD-related concepts, recent updates of several imaging guidelines aim to optimize the approach to ILD. Artificial intelligence tools are promising adjuncts to the qualitative CT assessment and will likely augment the role of CT in the ILD realm.

© RSNA, 2025

Supplemental material is available for this article.

Interstitial lung disease (ILD) is a heterogeneous group of diffuse parenchymal lung disorders characterized by varying degrees of chronic inflammation, fibrosis, or both, which may progress to respiratory failure. The use of thin-section chest CT has allowed a greater understanding of various ILD manifestations. Increased appreciation of radiologic-pathologic correlation and risks associated with surgical lung biopsy have shifted the diagnostic paradigm from a histopathology-based approach to a noninvasive, multidisciplinary approach heavily reliant on imaging. Aided by multidisciplinary discussion, CT achieves high-confidence diagnosis in most patients (1). The increased recognition of prognostic imaging markers in ILD and the recent expansion of antifibrotic therapy beyond idiopathic pulmonary fibrosis (IPF) have placed a greater emphasis on the role of CT in ILD. Importantly, the identification of fibrosis carries direct prognostic and therapeutic implications. With mounting understanding, ILD diagnosis continuously evolves, as reflected by the recent updates of several imaging guidelines and the emergence of novel ILD-related concepts. However, ILD diagnosis remains complex because clinical, imaging, and pathologic manifestations of different ILDs may overlap. Despite thorough multidisciplinary discussion, a substantial minority of patients have unclassifiable ILD (2). In this review, we discuss current and emerging concepts of ILD imaging with an emphasis on usual interstitial pneumonia (UIP), a specific histologic and radiologic lung fibrosis pattern, and suggest a UIP-centric approach of fibrotic ILD, aimed at guiding the approach to ILD. Artificial intelligence (AI) tools, promising adjuncts of qualitative CT assessment, will likely augment the role of CT in the ILD realm.

## Thin-Section Chest CT: Technical Evolution and Current Considerations

Multidetector volumetric CT using single breath-hold, contiguous, thin-section imaging of the thorax has substantially increased

the diagnostic value of CT in diffuse lung diseases, largely supplanting sequential CT (3,4). Thin-section CT technique is critical for the assessment of ILD. Owing to increased temporal and spatial resolution, volumetric thin-section CT reduces volume averaging and motion artifact, thereby optimizing the characterization of fine parenchymal detail and increasing sensitivity to subtle abnormality. It allows for thin-section multiplanar reconstructions ( $\leq 1.5$  mm; typically, 1 mm or 1.25 mm), contributing to a more efficient and possibly more accurate determination of the cranio-caudal distribution of abnormality. A moderate edge-enhancing reconstruction kernel (for example, Siemens B45f, GE Bone, Philips D or YB, and Toshiba Lung Std) is recommended to maximize spatial resolution while minimizing excessive noise (4,5). Iterative reconstruction aids dose optimization and noise reduction, with improved signal-to-noise ratio compared with filtered back projection. However, it should be used cautiously, as excessive iterative reconstruction can cause oversmoothing, potentially obscuring subtle ILD manifestations (6,7). Recommended CT parameters for ILD assessment are summarized in Table S1.

## The Rationale behind A UIP-Centric Imaging Approach

Current ILD practice guidelines are based on a growing body of literature examining the clinical significance of CT findings and their histologic correlation (8,9). The high prevalence of UIP in IPF, strong radiologic-pathologic correlation of UIP, and prognostic and therapeutic implications of a timely UIP diagnosis provide the rationale for a UIP-centric imaging approach. A simplified approach is summarized in Figure 1 and detailed in this review.

## UIP in IPF Diagnosis

In 2013, the second iteration of the American Thoracic Society (ATS) and European Respiratory Society (ERS) classification of

## Abbreviations

ACCP = American College of Chest Physicians, AI = artificial intelligence, ALAT = Asociación Latinoamericana de Tórax, ATS = American Thoracic Society, CPFE = combined pulmonary fibrosis and emphysema, ERS = European Respiratory Society, GGO = ground-glass opacity, HP = hypersensitivity pneumonitis, IIP = idiopathic interstitial pneumonia, ILA = interstitial lung abnormality, ILD = interstitial lung disease, IPF = idiopathic pulmonary fibrosis, JRS = Japanese Respiratory Society, PPF = progressive pulmonary fibrosis, UIP = usual interstitial pneumonia

## Summary

Given the paramount importance of CT in the diagnosis, prognosis, and monitoring of interstitial lung disease (ILD), particularly fibrotic ILD, radiologists should familiarize themselves with current imaging guidelines and emerging ILD-related concepts.

## Essentials

- Interstitial lung disease (ILD) is a heterogeneous group of diffuse parenchymal lung disorders, characterized by varying degrees of chronic inflammation, fibrosis, or both, that relies on a multidisciplinary approach for diagnosis, aided by thin-section chest CT ( $\leq 1.5$  mm).
- Beyond diagnosis, CT has also become essential for ILD prognostication and follow-up, aiding the identification of fibrotic and progressive forms.
- The presence of fibrosis in ILD is a critical determinant of prognosis, particularly when typical features of usual interstitial pneumonia (UIP), a specific histologic and radiologic lung fibrosis pattern, are identified.
- The prevalence of UIP, its prognostic implications, and its strong radiologic-pathologic correlation in idiopathic pulmonary fibrosis provide the rationale for a UIP-centric approach, guided by current imaging guidelines.
- Early identification of interstitial lung abnormality, recognition of prognostic imaging markers, and progressive pulmonary fibrosis in established ILD can guide management and help optimize patient prognosis.

idiopathic interstitial pneumonias (IIPs) grouped these entities into chronic fibrosing IIPs, smoking-related IIPs, acute or sub-acute IIPs, and rare IIPs (10,11). IPF—a chronic fibrosing IIP—is the most common fibrotic ILD and is characterized by a UIP pattern at CT and histologic examination (2,12).

The Fleischner Society white paper and 2022 clinical practice guidelines of the ATS, European ERS, Japanese Respiratory Society (JRS), and Asociación Latinoamericana de Tórax (ALAT) (hereafter, ATS/ERS/JRS/ALAT) define four diagnostic CT categories for UIP associated with a decremental likelihood of histologic UIP: typical UIP (Fleischner Society) or UIP (ATS/

ERS/JRS/ALAT), probable UIP, indeterminate for UIP, and alternative diagnosis (4,13,14) (Table 1).

**Typical UIP and probable UIP.**—Typical UIP and probable UIP are defined at CT as subpleural and basilar predominant fibrosis characterized by reticulation, traction bronchiectasis and/or bronchiolectasis, and absence of features suggesting an alternative diagnosis (Fig 2). Other possible features of UIP include the presence of mild ground-glass opacity (GGO), some upper lobe involvement, and heterogeneity of peripheral fibrosis with lobular distortion (15). Honeycombing is a distinguishing feature of typical UIP and absent in probable UIP. Honeycombing at CT is the most specific finding of UIP. One should remember that imaging patterns can change over time. For instance, a nonspecific interstitial pneumonia pattern can occasionally evolve into a typical UIP pattern over many years (16,17).

**Indeterminate for UIP.**—When high confidence cannot be reached for UIP or alternative diagnoses, the pattern is deemed indeterminate for UIP, particularly if the distribution of fibrosis is very mild or slightly atypical.

**Alternative diagnosis.**—When the findings or distribution are suggestive of a non-UIP entity, an alternative diagnosis is favored (Table 1; Figs 1, 3). This includes patterns characterized by subpleural sparing, upper or mid lung predominance and/or perilymphatic or peribronchovascular predominance, and those where cysts, mosaic attenuation, extensive GGO, consolidation, or nodules are dominant features. If alternative features are present, it is important to ensure that they are part of the underlying ILD rather than a superimposed acute process such as infection, aspiration, or edema. When compared with the 2018 version, the 2022 ATS/ERS/JRS/ALAT guidelines specify ranges of confidence levels for UIP histologic characteristics and introduce minor changes pertaining to the radiologic description of the

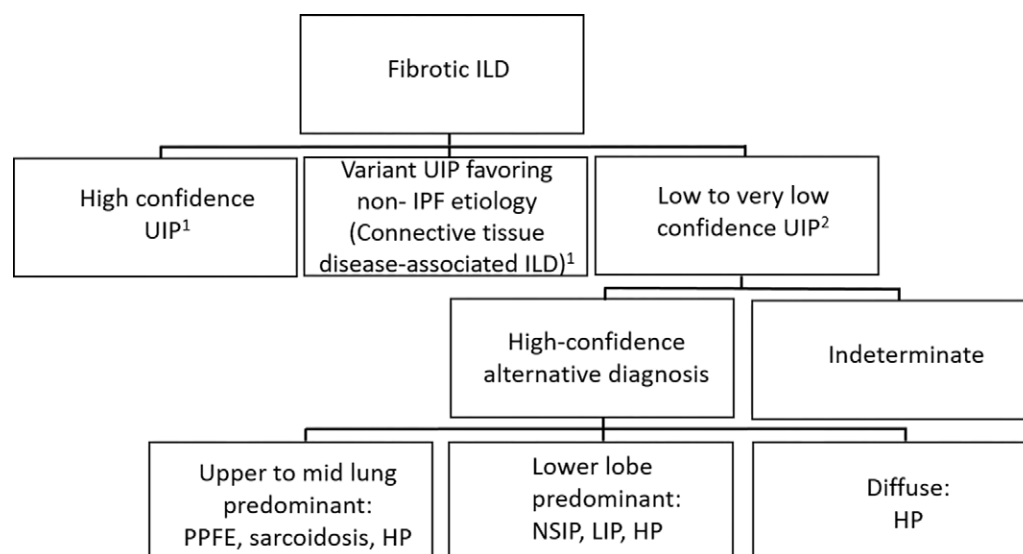


**Figure 1:** Diagram depicts a simplified approach to fibrotic interstitial lung disease (ILD) at CT. 1 = Clinical assessment is performed to confirm or exclude secondary usual interstitial pneumonia (UIP). 2 = Clinical assessment and histopathologic examination are performed when appropriate to confirm and investigate alternative diagnoses to UIP in idiopathic pulmonary fibrosis (IPF). HP = hypersensitivity pneumonitis, LIP = lymphocytic interstitial pneumonia, NSIP = nonspecific interstitial pneumonia, PPFE = pleuroparenchymal fibroelastosis.

**Table 1: Summary of the Diagnostic UIP Categories as Defined by the ATS/ERS/JRS/ALAT Guidelines**

Parameter	UIP	Probable UIP	Indeterminate for UIP	Alternative Diagnosis*
Confidence (%) <sup>†‡</sup>	>90	70–89	51–69	≤50
Predominant distribution	Subpleural Basal Possibly asymmetric <sup>‡</sup>	Subpleural No subpleural sparing <sup>‡</sup> Basal	Diffuse	Peribronchovascular Subpleural sparing <sup>‡</sup> Perilymphatic Upper lung Mid lung
Dominant imaging features	Honeycombing With or without traction bronchiectasis and/or bronchiolectasis Mild reticulation <sup>‡</sup> Irregular interlobular septal thickening <sup>‡</sup>	No honeycombing Traction bronchiectasis and/or bronchiolectasis Reticulation	Nonspecific features	Cysts Mosaicism Three-density sign GGO Nodules (including profuse CLN) Consolidation
Additional possible imaging features	Mild GGO <sup>‡</sup> DPO <sup>‡</sup>	Mild GGO		Pleural plaques Esophageal dilatation

Source.—Reference 13.

Note.—ALAT = Asociación Latinoamericana de Tórax, ATS = American Thoracic Society, CLN = centrilobular nodules, DPO = dendriform pulmonary ossification, ERS = European Respiratory Society, GGO = ground-glass opacity, JRS = Japanese Respiratory Society, UIP = usual interstitial pneumonia.

\* Distal clavicular erosions and extensive lymphadenopathy were ancillary imaging features included in the 2018 guidelines and omitted in the updated guidelines.

<sup>†</sup> Diagnostic confidence for histologic UIP.

<sup>‡</sup> Additions in the most recent ATS/ERS/JRS/ALAT guidelines, relative to the 2018 guidelines.

diagnostic categories, including a more detailed description of UIP and probable UIP (Table 1) (4,13).

### Radiologic-Pathologic Correlation of UIP

The relevance of the diagnostic UIP imaging categories lies in their ability to serve as histologic correlates. The reported positive predictive values for histologic UIP in typical UIP and probable UIP CT patterns exceed 90% and 80%, respectively (12,18). The prevalence of IPF and the presence of substantial traction bronchiectasis were, however, primary determinants of the positive predictive value of probable UIP in a prior report (19). Although UIP is the radiologic and histologic hallmark of IPF, it is not specific for IPF and can be associated with other diagnoses, including connective tissue disease-associated ILD, fibrotic hypersensitivity pneumonitis (HP), familial pulmonary fibrosis, Hermansky-Pudlak syndrome, and asbestosis.

When a UIP pattern is identified at CT, a thorough clinical assessment is critical to determine the likelihood of IPF and to exclude other fibrotic ILDs. Older age, male sex, and a smoking history confer a higher risk of IPF (14,20,21). The diagnosis of IPF is confirmed through multidisciplinary discussion when UIP or probable UIP are identified at CT and possible secondary causes have been excluded, thereby obviating the need for biopsy (13,14,22). In contrast, tissue sampling may be necessary for indeterminate or alternative CT patterns of fibrotic ILD as histologic UIP may be present in up to 60% of these cases (10,12).

### Prognosis of UIP

The identification of UIP features at CT carries important prognostic implications, emphasizing the role of imaging

in patient risk stratification and outcome optimization. The timely initiation of antifibrotic therapy in select patients reduces lung function decline and improves survival (23,24). High-confidence radiologic and histologic UIP patterns consistently portend worse prognosis with greater progression and shorter survival when compared with indeterminate and alternative patterns of fibrosis, even in non-IPF etiologies (9,10,18,25,26). Honeycombing—the key distinguishing imaging feature of UIP from probable UIP—constitutes an independent adverse prognostic imaging marker (25,27). Concordant with these findings, a survival advantage and a lower risk of acute exacerbation is described in probable UIP versus UIP at CT (28,29). Traction bronchiectasis and a greater extent of fibrosis at CT are predictive of adverse outcomes in IPF irrespective of the confidence level for UIP at CT (30). Interestingly, traction bronchiectasis and honeycombing are currently thought to reflect a spectrum of severity of airway distortion. In IPF, honeycombing at CT is now thought likely to represent end-stage peripheral traction bronchiolectasis, which results from alveolar collapse and fibrosis (13,31,32). These findings underline the importance of accurate terminology in ILD with detailed characterization of fibrotic features, including adverse prognostic markers when present. The evolving understanding of IPF has been paralleled by the emergence of novel terminology and concepts in ILD imaging, which are discussed in the following sections of this review.

### Secondary UIP

Secondary UIP refers to the UIP pattern observed in conditions other than IPF. Although IPF is the most common cause of



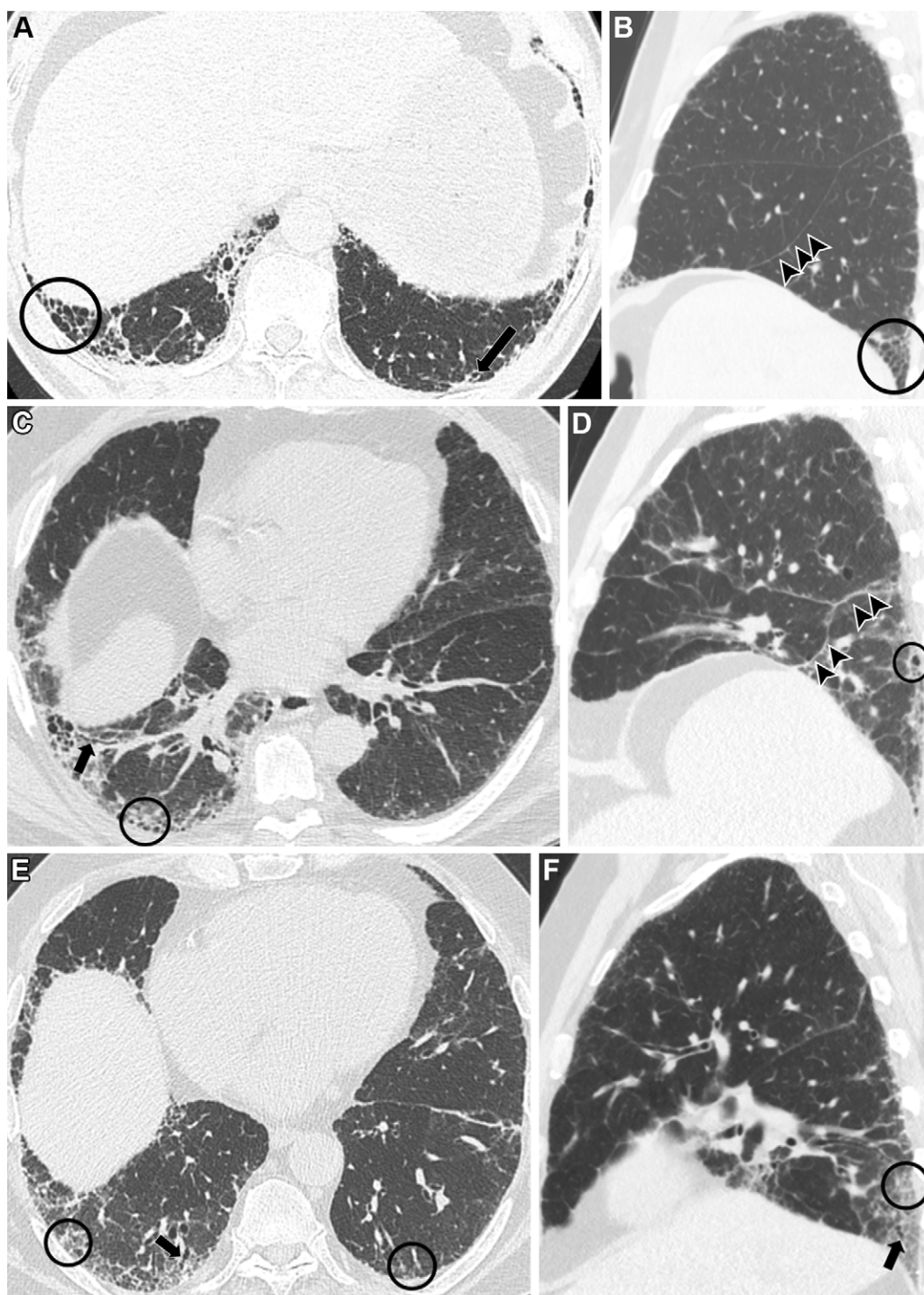


**Figure 2:** Images in two patients with idiopathic pulmonary fibrosis (IPF) and high-confidence usual interstitial pneumonia (UIP) diagnosis at chest CT. Unenhanced **(A)** axial and **(B)** sagittal CT images in a 68-year-old male with UIP at CT show lower lobe–predominant fibrosis characterized by honeycombing superimposed on reticulation (circles), subtle traction bronchiolectasis (arrow in **A**), and lower lobe volume loss as demonstrated by mild posterior retraction of the right major fissure (arrowheads in **B**). Unenhanced **(C)** axial and **(D)** sagittal CT images in a 77-year-old male with asymmetric UIP pattern at CT show asymmetric fibrosis characterized by asymmetric right lower lobe–predominant honeycombing superimposed on reticulation (circles), traction bronchiectasis and/or bronchiolectasis (arrow in **A**), and right lower lobe volume loss. The right major fissure is distorted posteriorly and inferiorly displaced (arrowheads in **D**). Unenhanced **(E)** axial and **(F)** sagittal CT images in a 66-year-old male with probable UIP pattern at CT show lower lobe–predominant fibrosis characterized by reticulation (circles) and traction bronchiectasis and/or bronchiolectasis (arrow). The findings are also asymmetrically greater on the right.

UIP at CT, accounting for approximately two-thirds of cases (16,33), the UIP pattern may be associated with other disorders, including connective tissue disease–associated ILD, familial pulmonary fibrosis, fibrotic HP, and other exposure-related

disorders (34,35). Although CT findings of secondary UIP can mimic IPF, CT can commonly suggest a secondary cause. As per the current ATS, JRS, and ALAT (hereafter, ATS/JRS/ALAT) HP imaging guidelines, a UIP pattern of fibrosis



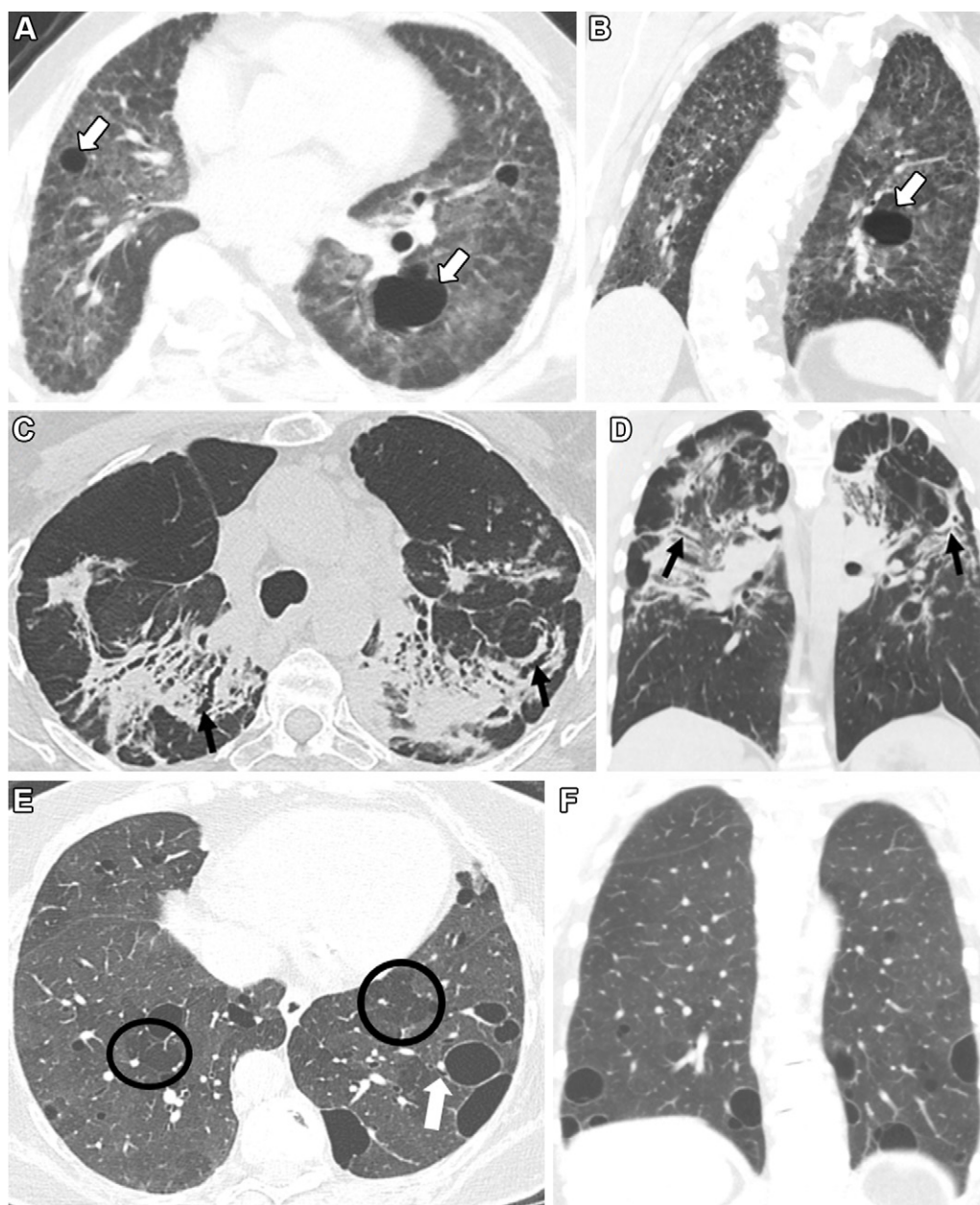


**Figure 3:** Images in three patients with low to very low confidence usual interstitial pneumonia (UIP) diagnosis at CT. Unenhanced (A) axial and (B) coronal CT images in a 39-year-old male with familial pulmonary fibrosis show diffuse ground-glass opacity and reticulation and scattered cysts (arrows), indeterminate for UIP. Unenhanced (C) axial and (D) coronal CT images in a 58-year-old female with sarcoidosis show upper and perihilar predominant fibrosis characterized by peribronchovascular opacity, traction bronchiectasis (arrows), and architectural distortion. Unenhanced (E) axial and (F) coronal CT images in a 73-year-old female with Sjögren syndrome show lower lobe- and perivascular-predominant cysts closely associated with bronchovascular bundles (arrow in E), and with mosaic attenuation (circles in E). Findings are strongly suggestive of an alternative etiology to UIP and are compatible with lymphocytic interstitial pneumonia.

associated with features of small airway disease (eg, centrilobular nodules with ground-glass attenuation, three-density sign, air trapping, or some combination thereof) is in favor of an alternative diagnosis to IPF and may be compatible with fibrotic HP (Fig 4). Asbestosis also typically manifests as UIP at CT and is suspected when asbestos-related pleural plaques are present (Fig 4) (13). Other common ancillary findings in asbestosis include mosaic attenuation and subpleural dot-like or branching nodules (36,37). Asbestosis is characterized by a more insidious disease course with slower clinical and radiologic progression when compared with IPF (38).

#### Variant UIP in Connective Tissue Disease–associated ILD

With connective tissue disease–associated ILD, distinct UIP patterns at CT occasionally termed *variant* or *UIP-like* patterns are increasingly recognized (16,39–41) (Table 2, Fig 5). Imaging findings suggestive of connective tissue disease–associated ILD include exuberant honeycombing involving more than 70% of the fibrotic lung, disproportionate involvement of the anterior segments of the upper lobes (anterior upper lobe sign), and horizontal demarcation of fibrosis from adjacent normal lung on coronal reformatted images (straight-edge sign) (16). Of these, the straight-edge sign has the

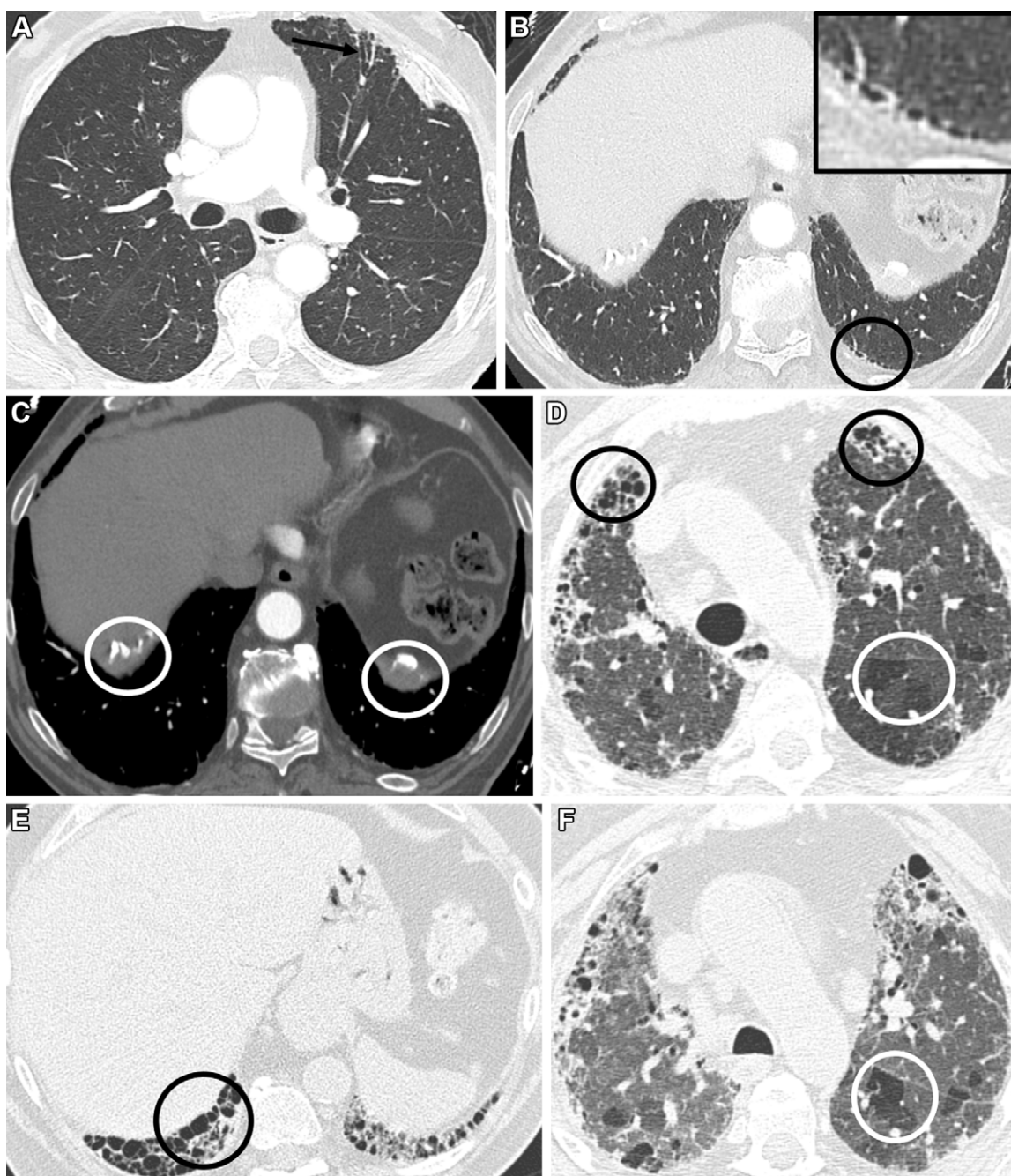


**Figure 4:** Images of secondary usual interstitial pneumonia in two patients. **(A, B)** Unenhanced axial CT images in lung window in a 70-year-old male with asbestosis show left upper lobe bronchiectasis and/or bronchiolectasis associated with mild subpleural reticulation (arrow in **A**) and mild left lower lobe honeycombing (circle in **B**; inset image). **(C)** Unenhanced axial CT image in soft tissue window shows partially calcified pleural plaques (circles) compatible with asbestos-related pleural disease. Unenhanced **(D, E)** inspiratory and **(F)** expiratory axial CT images in lung window in a 68-year-old female with fibrotic hypersensitivity pneumonitis show anterior upper lobe– and posterior lower lobe–predominant honeycombing (black circles in **D** and **E**). Multifocal mosaic attenuation and corresponding air trapping (white circle in **D** and **F**) support an alternative diagnosis to idiopathic pulmonary fibrosis.

highest specificity (16,41). Other findings described in certain connective tissue disease–associated ILDs are unlikely to be specific for a single disease, although their association with various disease types remains unexplored (40). For example, a disproportionate involvement of the anterolateral upper and posterosuperior lower lobes is described in systemic sclerosis (four corners sign). Areas of wedge-shaped UIP-like fibrosis (ie, island-like fibrosis) or admixed regional GGO, nonhoneycomb cysts, and reticulation (heterogeneous lung destruction) are described in systemic lupus erythematosus, although UIP

in isolated systemic lupus erythematosus is rare (39,42). Detailed assessment of previous imaging is critical. In island-like fibrosis, early examinations may show corresponding GGO or consolidation (39). Overlapping fibrotic patterns (eg, overlapping UIP and nonspecific interstitial pneumonia) and longitudinal progression from non-UIP to overlapping or UIP and/or UIP-like patterns strongly suggest connective tissue disease–associated ILD (43) (Fig 6). Ancillary imaging signs can also aid this diagnosis. These include esophageal dilatation and severe pulmonary hypertension in systemic sclerosis, and

**Table 2: Chest CT Signs Described as “Variant” or “UIP-like” Patterns and Favoring Secondary UIP due to Connective Tissue Disease–associated ILD over UIP in IPF**

Imaging Sign	Description	Initial Description
Exuberant honeycombing	Stacked cysts abutting the pleura and involving more than 70% of the fibrotic lung	Connective tissue disease–associated ILDs: RA, SSc, MCTD, Sjögren syndrome, myositis
Straight-edge sign	Sharp horizontal delineation of fibrosis from relatively spared parenchyma in the coronal reconstruction, without superior extension laterally	Connective tissue disease–associated ILDs: RA, SSc, MCTD, Sjögren syndrome, myositis
Anterior upper lobe sign	Disproportionate involvement by fibrosis of the anterior segments in the upper lobes	Connective tissue disease–associated ILDs: RA, SSc, MCTD, Sjögren syndrome, myositis
Four corners sign	Disproportionate involvement by fibrosis of the anterolateral upper lobes and posterosuperior lower lobes	SSc
Heterogeneous lung destruction	Confluent regions of combined GGO, nonhoneycomb cysts, and reticulation	SLE
Island-like fibrosis	Focal wedge-shaped honeycombing and reticulation with angular margins to the pleura	SLE

Source.—References 16, 39, and 42.

Note.—GGO = ground-glass opacity, ILD = interstitial lung disease, IPF = idiopathic pulmonary fibrosis, MCTD = mixed connective tissue disease, RA = rheumatoid arthritis, SLE = systemic lupus erythematosus, SSc = systemic sclerosis, UIP = usual interstitial pneumonia.

bony erosions and necrobiotic nodules in rheumatoid arthritis–associated ILD (43).

### Important ILD Entities beyond UIP

Growing evidence has also driven changes to the diagnostic and management approach of non-IPF fibrotic ILDs. Updated clinical practice guidelines and official research statements notably provide a framework for the diagnosis of HP, combined pulmonary fibrosis and emphysema, and progressive pulmonary fibrosis, discussed in the following section.

#### Hypersensitivity Pneumonitis

HP refers to a heterogeneous group of ILDs resulting from the recurrent exposure to inhaled antigens in susceptible hosts (44). Current practice guidelines aim at streamlining the diagnosis and management of these diseases, made challenging by their geographic and clinical heterogeneity and a large variety of potential inciting pathogens. Reports demonstrating the prognostic significance of fibrosis in HP have provided the basis for a dual nomenclature reliant on the presence or absence of fibrosis in the current ATS/JRS/ALAT and American College of Chest Physicians (ACCP) guidelines (Tables 3, 4) (45,46). The previous temporal nomenclature has been abandoned because acute, subacute, and chronic HP categories frequently overlapped and failed to reflect prognosis (34,44,47,48).

In these imaging guidelines, CT is the primary step in determining the overall clinical confidence in the diagnosis of HP and in distinguishing fibrotic from nonfibrotic HP. This distinction is critical for prognosis and management. In both guidelines, to reflect the level of diagnostic confidence for HP, findings at CT are categorized as typical for HP or compatible with HP in nonfibrotic forms and as typical for HP, compatible with HP, or indeterminate for HP in fibrotic forms (34,47). A typical HP pattern at CT is highly specific for this diagnosis (49).

Variable distributions of abnormality and patterns of fibrotic HP are detailed in the ATS/JRS/ALAT guidelines, in contrast to the ACCP guidelines. In the ATS/JRS/ALAT guidelines,

high-confidence diagnosis requires the association of parenchymal opacity, fibrosis, or both with features of small airways disease (Figs 7, 8; Table 3) (34). The craniocaudal distribution of findings in high-confidence HP categories may be diffuse or may show upper, mid, or lower lung predominance. In the axial plane, peribronchovascular or subpleural predominance may be seen. Parenchymal opacities consist mainly of GGOs or mosaic attenuation. Fibrosis is primarily characterized by coarse reticulation. Honeycombing and traction bronchiectasis can be present. The three-density pattern or sign (Fig 7) is highly specific for HP and defined as the juxtaposition of regional parenchymal hypoattenuation, normal attenuation, and hyperattenuation (50). This term is limited to fibrotic HP in the ATS/JRS/ALAT guidelines.

Conversely, the three-density sign is accepted in nonfibrotic and fibrotic HP in the ACCP guidelines. Hypoattenuating areas correlate with air trapping on expiratory images. Hyperattenuating (ground glass) areas correlate with parenchymal infiltration and/or fibrosis. Regions of normal attenuation correspond to interspersed spared parenchyma. Imaging features of small airways disease include air trapping resulting from small airway obstruction or centrilobular ground-glass nodules resulting from airway-centered inflammation or peribronchiolar fibrosis (51). When small airways disease is a dominant CT feature, a diagnosis of HP should be favored. In cases with conflicting or overlapping CT features of fibrotic HP and UIP, the findings should be integrated with clinical probabilities (52). Relevant to mosaic attenuation, the presence of a minimum of five hypoattenuating lobules in a minimum of three lobes may aid in distinguishing HP from UIP in IPF, although the assessment of mosaic attenuation in clinical practice remains largely subjective (53).

In the ACCP guidelines, typical HP could manifest solely with diffuse centrilobular nodules or with mosaic attenuation and either air trapping and centrilobular nodules or the three-density sign (Figs 7, 8; Table 4) (47). Features suggestive of alternative diagnoses are absent in typical and compatible HP



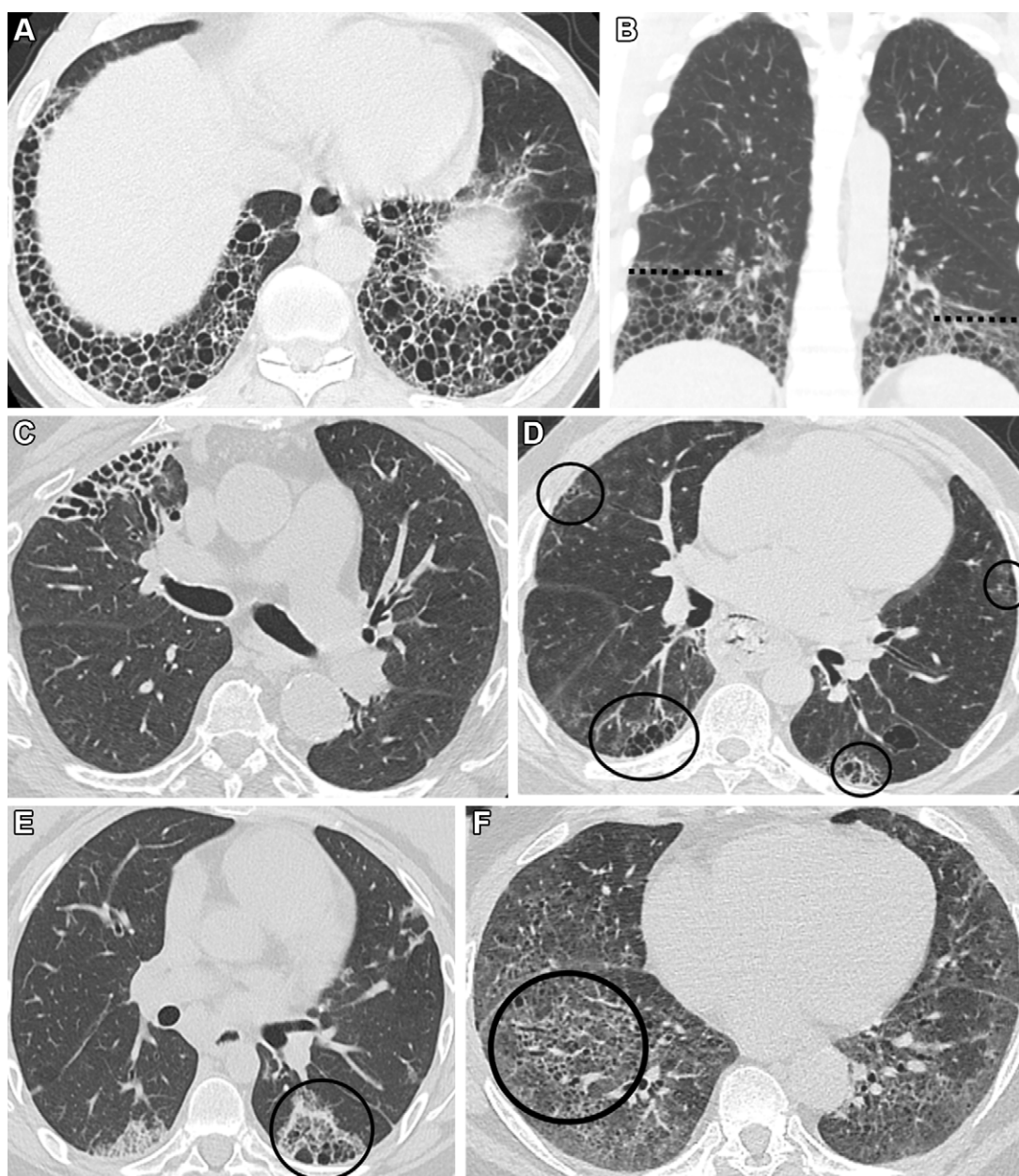


**Figure 5:** Images depict CT signs of connective tissue disease–related interstitial lung disease (ILD) in five patients. Unenhanced (A) axial and (B) coronal CT images in a 62-year-old male with mixed connective tissue disease–related ILD show exuberant honeycombing of the lower lobes, with a straight-edge sign on coronal reformatted image (dashed lines in B). (C) Unenhanced axial CT image in a 72-year-old female with rheumatoid arthritis–related ILD shows asymmetric involvement of the anterior right upper lobe with focal honeycombing and reticulation (ie, anterior upper lobe sign). (D) Unenhanced axial CT image in a 45-year-old male with systemic sclerosis–related ILD shows multifocal honeycombing and reticulation disproportionately involving the anterolateral upper and posterolateral lower lobes (ie, four corners sign) (circles). (E) Unenhanced axial CT image in a 20-year-old female with systemic lupus erythematosus shows focal wedge-shaped area of usual interstitial pneumonia–like fibrosis of the superior left lower lobe, with honeycombing and reticulation (circle). (F) Unenhanced axial CT image in a 57-year-old female with antisynthetase syndrome shows admixed ground-glass opacity, reticulation, and cysts within the visualized lungs (ie, heterogeneous lung destruction sign) (circle).

patterns. In both guidelines, findings are usually less extensive in compatible patterns when compared with typical patterns.

**Important practical tips and pitfalls of HP imaging and diagnosis.**—HP cannot be excluded on the basis of imaging alone and should be considered in any patient with ILD. Imaging manifestations are broad and may overlap with other ILDs (34,44). Findings of “typical fibrotic HP” may notably be found in patients with connective tissue disease due to concomitant

small airway obstruction (52). In non-fibrotic HP, imaging findings may be subtle or even absent (54). The diagnosis should be guided by multidisciplinary discussion encompassing a thorough clinical and radiologic assessment and a review of bronchoalveolar lavage and histopathologic results when available. The diagnostic approach at CT should account for disease prevalence, which may impact the diagnostic performance of guidelines schemes. In a recent report, the accuracy of the ATS/JRS/ALAT guidelines was greater in low-prevalence environments

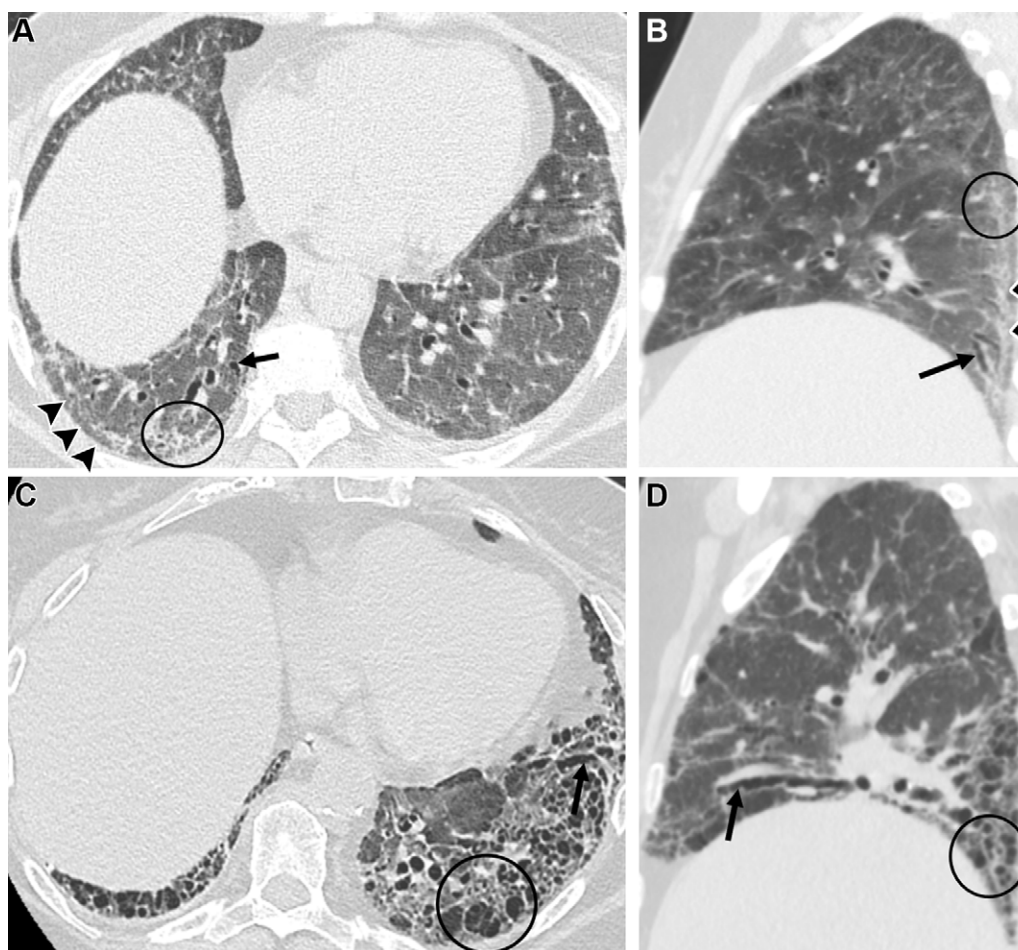


**Figure 6:** Images show the longitudinal progression from nonspecific interstitial pneumonia to variant usual interstitial pneumonia in a 70-year-old female with mixed connective tissue disease–related interstitial lung disease. Unenhanced (A) axial and (B) sagittal CT images from baseline chest CT show lower lobe– and peripheral–predominant reticulation (circle) superimposed on ground-glass attenuation, with subpleural sparing (arrowheads) and traction bronchiectasis and/or bronchiolectasis (arrow). Unenhanced (C) axial and (D) sagittal CT images obtained 13 years after initial evaluation show interval development of lower lobe–predominant exuberant honeycombing (circle) with progressed traction bronchiectasis (arrow) and new subpleural involvement.

and lower in high-prevalence environments compared with the ACCP guidelines (49). The simpler, more approachable ACCP classification could be more appealing for radiologists in general practice, where subspecialty ILD expertise is not available.

### Combined Pulmonary Fibrosis and Emphysema

Combined pulmonary fibrosis and emphysema (CPFE) remains a somewhat controversial entity and was originally defined as the combination of upper lobe–predominant emphysema and lower lobe–predominant fibrosis. CPFE is characterized by a distinct pulmonary function profile and worse prognosis when compared with IPF and emphysema alone (55–57). CPFE manifests as significantly impaired gas exchange with marked reduction in the diffusing lung capacity for carbon monoxide and normalized spirometry owing to concurrent obstructive and restrictive processes. Lung volumes are higher in CPFE when compared with IPF alone (55,58,59). Poor prognosis and lower life expectancy are associated with an increased risk of pulmonary hypertension, which occurs in up to half of patients (58). Consequently, CPFE is described as a syndrome, which can be suggested at imaging but should be corroborated with the clinical assessment (55). Although initially described at CT

as the combination of lower lobe–predominant UIP and upper lobe–predominant emphysema (ie, “strict” CPFE), a wider range of imaging manifestations is now accepted (Fig 9). Paraseptal and centrilobular emphysema are highly prevalent (55). Fibrosis is most commonly subpleural. Honeycombing is the most common fibrotic feature, occurring in more than 95% of patients (58,59). GGO is more pronounced than in isolated IPF and may reflect fine fibrosis, nonspecific interstitial pneumonia, or associated smoking-related lung disease (including smoking-related interstitial fibrosis and desquamative interstitial pneumonia) (58,59).

The diagnosis and characterization of CPFE can be challenging in clinical practice. The broader radiologic definition of CPFE remains somewhat poorly defined. In 2022, an official research statement by the ATS/ERS/JRS/ALAT attempted to better delineate the syndrome (55). Several morphologic subtypes are described depending on the separation and progressive transition or admixture of emphysema and fibrosis. The prognostic implication of these subtypes has not been explored. Another report defined three distinct clinical subtypes associated with progressively increased mortality: an emphysema-dominant subtype characterized by greater obstruction at

**Table 3: Summary of the Imaging Guidelines of the American Thoracic Society, Japanese Respiratory Society, and Asociación Latinoamericana de Tórax for Fibrotic and Nonfibrotic HP**

HP Type	CT Features		
	Typical HP	Compatible with HP	Indeterminate for HP
<b>Fibrotic</b>			
Fibrosis features	Predominant coarse reticulation and/or irregular linear opacities Possible honeycombing and traction bronchiectasis	UIP pattern (with honeycombing and possible traction bronchiectasis) Subtle fibrosis and extensive GGO	Fibrosis without compelling features of HP: UIP or probable UIP; fibrotic NSIP; organizing pneumonia; indeterminate
Small airways disease	At least one of the following: Ill-defined CLN and/or GGO Mosaicism, three-density pattern, and/or air trapping	At least one of the following: Ill-defined CLN Three-density pattern and/or air trapping	Fibrosis without compelling features of HP: UIP or probable UIP; fibrotic NSIP; organizing pneumonia; indeterminate
Possible distribution	Diffuse (axially and craniocaudally) or Mid lung predominant or Basilar sparing	Craniocaudally: upper lung predominant Axially: peribronchovascular, subpleural	Fibrosis without compelling features of HP: UIP or probable UIP; fibrotic NSIP; organizing pneumonia; indeterminate
<b>Nonfibrotic HP</b>			
Parenchymal findings	At least one of the following: GGO Mosaicism	Nonspecific findings Uniform and subtle GGO Consolidation Cysts	NA
Small airways disease	At least one of the following: Ill-defined CLN Air trapping	NA	NA
Possible distribution	Diffuse (axially and craniocaudally)	Diffuse Variant distribution (lower lung predominant; peribronchovascular)	NA

Source.—Reference 34.

Note.—CLN = centrilobular nodules, GGO = ground-glass opacity, HP = hypersensitivity pneumonitis, NA = not applicable, NSIP = nonspecific interstitial pneumonia, UIP = usual interstitial pneumonia.

**Table 4: Summary of the Imaging Guidelines of the American College of Chest Physicians for Fibrotic and Nonfibrotic HP**

HP Type	CT Features		
	Typical HP*	Compatible with HP*	Indeterminate for HP
Fibrotic	Fibrosis and at least one of the following: Diffuse, profuse ill-defined CLN Mosaicism with three-density sign <sup>†</sup>	Fibrosis and at least one present: Nonprofuse ill-defined CLN Mosaicism and air trapping not meeting criteria for typical HP Patchy or diffuse GGO	Fibrosis without other compelling features of HP
Nonfibrotic	At least one of the following: Diffuse and profuse ill-defined CLN Mosaicism with air trapping and CLN Mosaicism with three-density sign <sup>†</sup>	At least one of the following: Nondiffuse and nonprofuse ill-defined CLN Patchy and diffuse GGO Mosaicism or air trapping not meeting criteria for typical HP	NA

Source.—Reference 47.

Note.—CLN = centrilobular nodules, GGO = ground-glass opacity, HP = hypersensitivity pneumonitis, NA = not applicable.

\* Patterns typical for HP and compatible with HP imply the absence of features suggestive of alternative diagnoses.

<sup>†</sup> The three-density sign is defined as the juxtaposition of regional parenchymal hypoattenuation, normal attenuation, and hyperattenuation.

spirometry and lower CT fibrosis scores, a non-IPF fibrotic-dominant type characterized by smaller lung volumes and lower CT emphysema scores, and, most commonly, an IPF-dominant subtype (ie, strict CPFE) characterized by severe restriction at spirometry and greater CT fibrosis scores (56). The recognition of UIP can be challenging when it is confounded by emphysema, particularly in admixed patterns (14). Recently, the use of delayed imaging at gadolinium-enhanced thoracic MRI has shown promise in distinguishing emphysema from fibrosis (60).

Because the umbrella term *CPFE* may obscure the heterogeneity of its radiologic appearances, it is probably best to separately describe the imaging features in each patient, including the predominant pattern of emphysema (centrilobular, paraseptal, etc) and the predominant pattern of fibrosis.

The coexistence of emphysema and pulmonary fibrosis is common and is not synonymous with CPFE. Emphysema and pulmonary fibrosis, particularly IPF, share common risk factors and common pathogenetic pathways influenced by genetic and



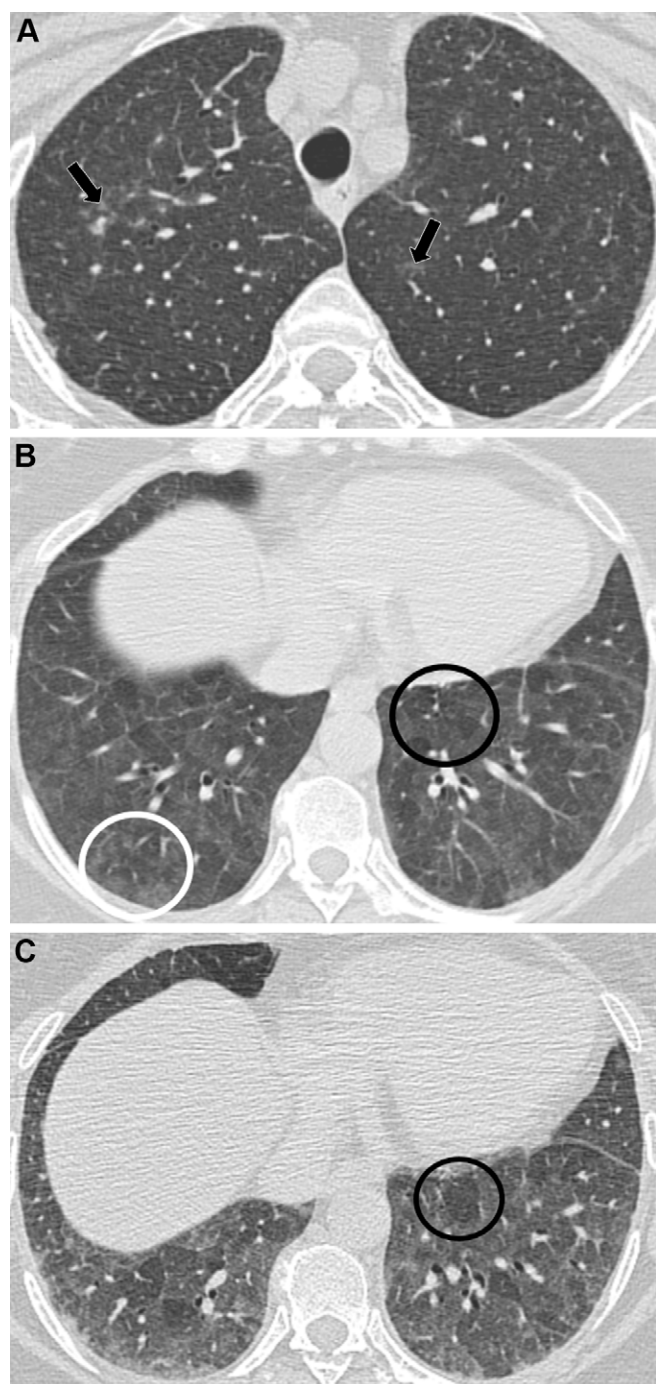


**Figure 7:** Images in a 58-year-old female with nonfibrotic hypersensitivity pneumonitis due to hot tub exposure. Unenhanced axial (**A**, **B**) inspiratory and (**C**) expiratory CT images show centrilobular nodules (arrows in **A**) and ill-defined ground-glass opacity (white circle in **B**) diffusely in the lungs, inspiratory mosaic attenuation (black circle in **B**), and air trapping (circle in **C**).

environmental factors (61). A majority of patients with IPF (60%–80%) have a history of smoking (62). Other shared risk factors include older age, male sex, occupational or inhalational exposures, and genetic polymorphisms (55). Smoking-related interstitial fibrosis is also common in smokers, characterized by airspace enlargement with alveolar septal fibrosis (63). In contrast with CPFE, clinical manifestations of smoking-related interstitial fibrosis are typically mild and nonprogressive. The

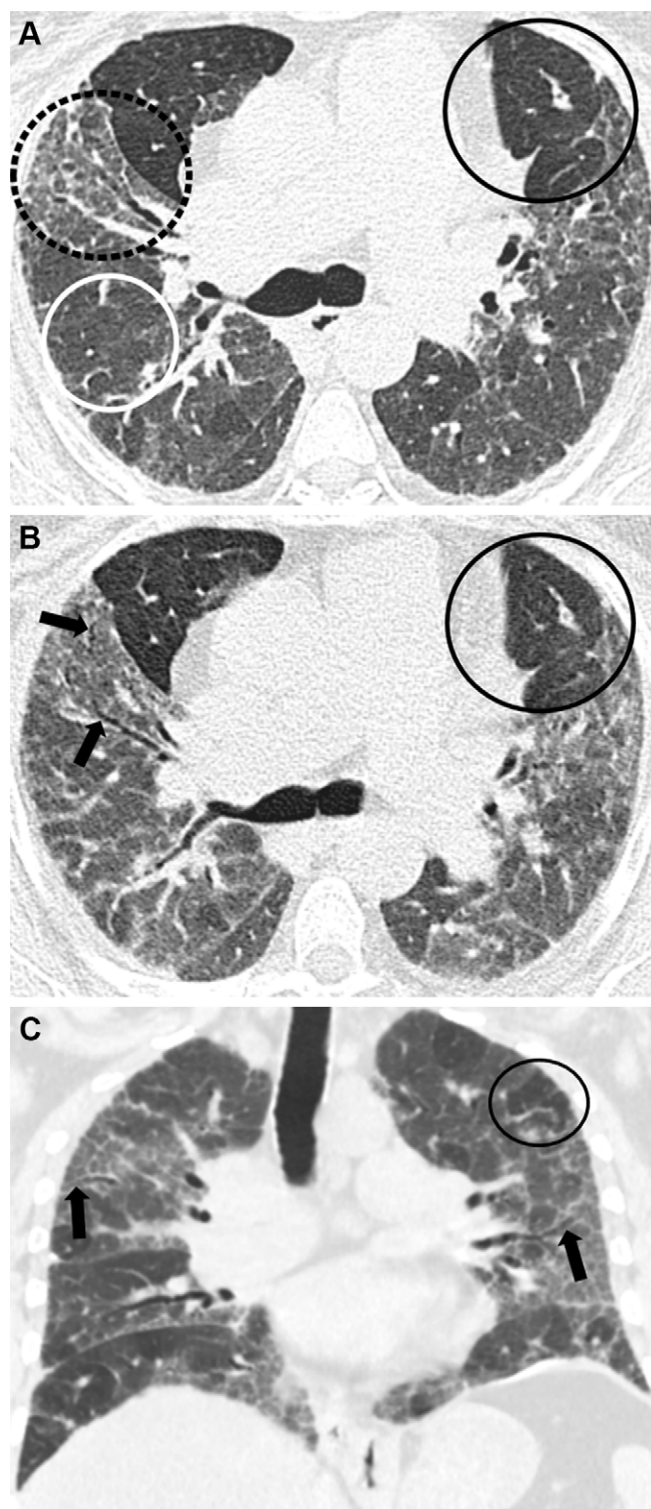


**Figure 8:** Images in a 57-year-old female with fibrotic hypersensitivity pneumonitis due to extensive mold exposure. Unenhanced (**A**) axial inspiratory, (**B**) axial expiratory, and (**C**) coronal inspiratory CT images show juxtaposed areas of ground-glass opacity (dashed circle in **A**), inspiratory mosaic attenuation (solid black circle in **A** and **C**) corresponding to expiratory air trapping (circle in **B**), and interspersed spared parenchyma (white circle in **A**) resulting in the three-density sign, defined as the juxtaposition of regional parenchymal hypoattenuation, normal attenuation, and hyperattenuation. There is associated reticulation and traction bronchiectasis (arrows in **B** and **C**). The pattern is typical for fibrotic hypersensitivity pneumonitis per the guidelines of the American College of Chest Physicians and the guidelines of the American Thoracic Society, Japanese Respiratory Society, and Asociación Latinoamericana de Tórax.

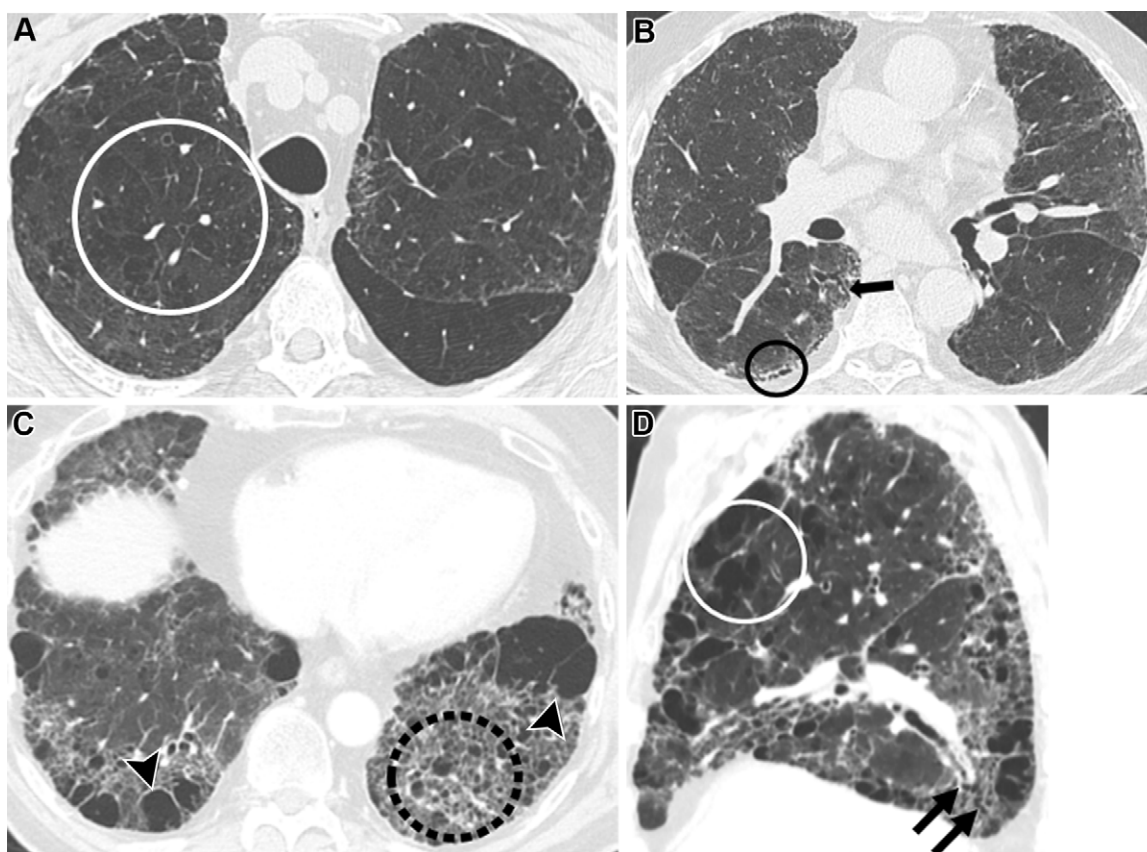


**Figure 9:** Images in two patients with combined pulmonary fibrosis and emphysema. Unenhanced (**A, B**) axial CT images in a 77-year-old male show upper lobe–predominant centrilobular emphysema (circle in **A** and **D**) and mild lower lobe usual interstitial pneumonia (UIP) fibrosis characterized by honeycombing (circle in **B**) and subtle traction bronchiolectasis (arrow in **B**). Unenhanced (**C**) axial and (**D**) sagittal CT images in a 60-year-old male show lower lobe–predominant non-UIP fibrosis characterized by reticulation, ground-glass attenuation, and cysts (circle in **C**) and traction bronchiectasis and/or bronchiolectasis (arrows in **D**) admixed with paraseptal emphysema and bullous change (arrowheads in **C**).

CT features of smoking-related interstitial fibrosis may include asymmetric confluent cysts of varying size with associated GGO and reticulation (64). Patients' clinical and functional profiles aid the differentiation of CPFE from concurrent emphysema and IPF and from smoking-related interstitial fibrosis.

### Progressive Pulmonary Fibrosis

Non-IPF fibrotic ILDs are progressive in up to 60% of patients (Fig 10) (65,66). Progressive pulmonary fibrosis (PPF) was recently formally defined to aid in the identification of these progressive phenotypes, allowing improved risk stratification and management guidance (12,65,66). PPF is described as the presence of at least two of the following criteria within a year of follow-up and despite appropriate management: (a) worsening respiratory symptoms, (b) deterioration of pulmonary function test results, and (c) progression of fibrosis at CT (13,65). This definition implies longitudinal follow-up subsequent to accurate diagnosis and treatment (65). The growing interest in PPF stems from recent trials showing a reduction in pulmonary function decline after treatment with antifibrotics for non-IPF ILDs (67). Although upfront antifibrotic therapy is not currently indicated in most patients, prognosis is optimized by early treatment when progression occurs (65). Given that the sensitivity of pulmonary function tests may be limited in detecting mild changes, the role of CT in the early identification of progression is emphasized

(68–70). CT can also help distinguish PPF from other etiologies of clinical deterioration such as treatment-related pneumonitis, infection, or acute ILD exacerbation (65,66). PPF may manifest with interval development, increased severity, or increased extent of honeycombing, reticulation, traction bronchiectasis and/or bronchiolectasis, or volume loss (66).

Increased GGO may also reflect progressive fibrosis. However, the differentiation from a superimposed acute process may be challenging and should be aided by the clinical context. Recommendations for follow-up CT are individualized (65). CT is recommended in patients with symptomatic or functional deterioration. Annual to biennial thin-section chest CT is appropriate in most clinically stable patients (65,66). Close monitoring should particularly be considered when honeycombing, traction bronchiectasis, or extensive fibrosis are present, as such findings confer a higher risk of progression (25,26,71,72). Honeycombing is associated with progression and increased mortality in various fibrotic ILDs, including connective tissue disease–associated ILD and fibrotic HP (26).

### Recent Advances and Future Directions in ILD Imaging

Promising developments in the ILD realm include the formal adoption of the terminology and general management paradigm for interstitial lung abnormalities (ILAs), and the expanded applications of quantitative tools in ILAs and ILD.



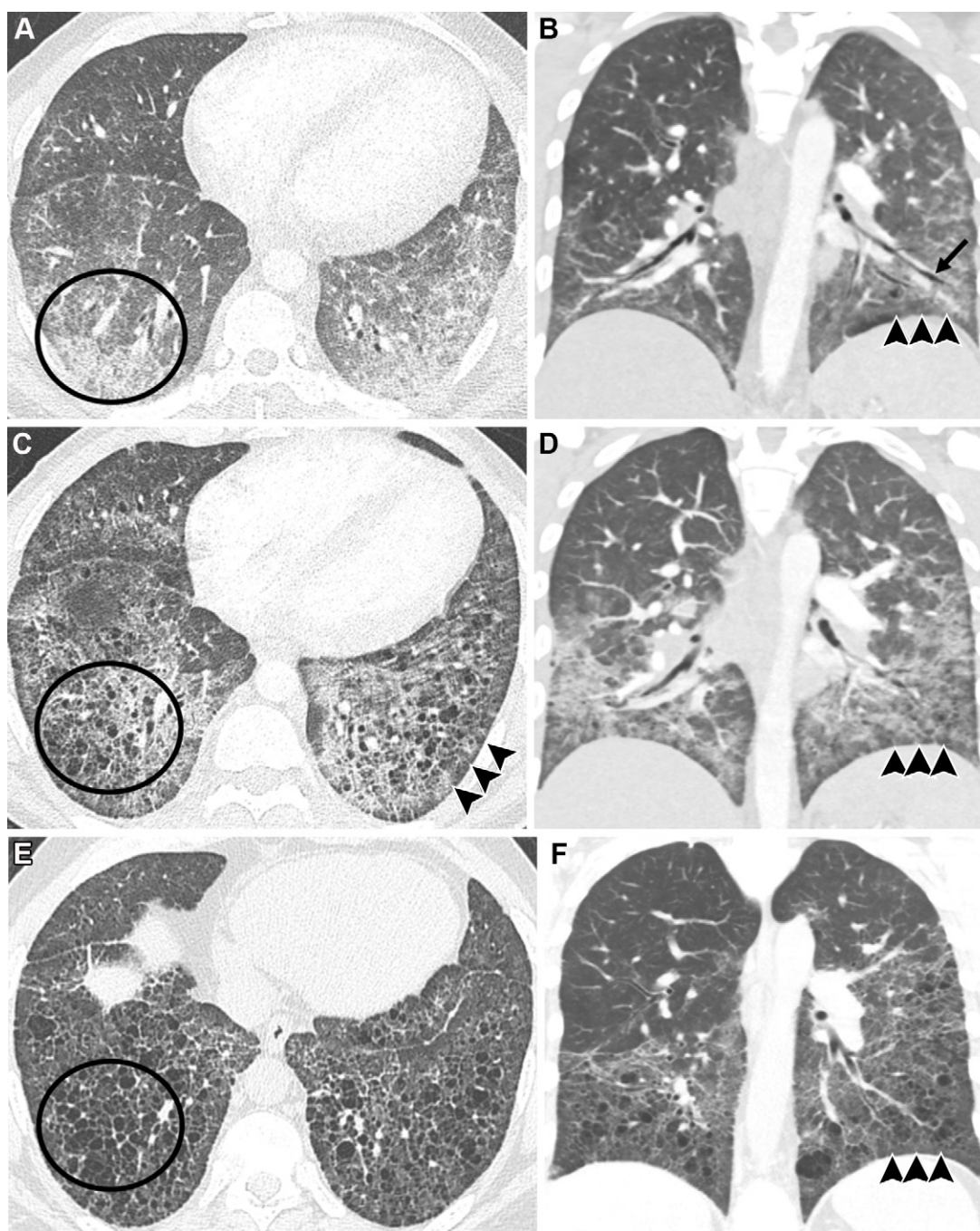


**Figure 10:** Images in a 36-year-old male with antisynthetase syndrome and progressive pulmonary fibrosis. Unenhanced (A) axial inspiratory and (B) coronal CT images from baseline chest CT show lower lobe–predominant ground-glass opacity and fine reticulation (circle in A) with mild traction bronchiectasis (arrow in B) and relative subpleural sparing (arrowheads in B), compatible with nonspecific interstitial pneumonia. Unenhanced (C) axial inspiratory and (D) coronal CT images from 6-month follow-up chest CT show increased extent of peribronchovascular predominant opacity and reticulation with new intermixed cysts, resulting in a “heterogeneous lung destruction” appearance (circle in C) and continued relative subpleural sparing (arrowheads in C and D). Unenhanced (E) axial inspiratory and (F) coronal CT images from 12-month follow-up chest CT show increased cysts superimposed on reticulation (circle in E), resolved opacities, and areas of continued relative subpleural sparing (arrowheads in F).

### Interstitial Lung Abnormalities

ILAs are incidental abnormalities of possible unsuspected, undiagnosed, or subclinical ILD at partial or complete CT of the chest. Although the ILA terminology was recently formally defined, the concept of early ILD recognition is not new (20,73). The recent accelerated interest in ILAs stems greatly from clinical trials showing a survival benefit accrued from the early initiation of antifibrotics in IPF and other progressive

fibrotic ILDs (13,74,75). ILAs are common and likely to be increasingly identified given trends in increased imaging use (20,76). ILAs are commonly progressive, although progression rates and follow-up periods are variable in former smoking and population-based smoking cohorts (20,76,77). ILAs are associated with increased respiratory symptoms, greater pulmonary functional impairment, and increased morbidity and mortality (21,78–80). Despite their potential implications, ILAs are



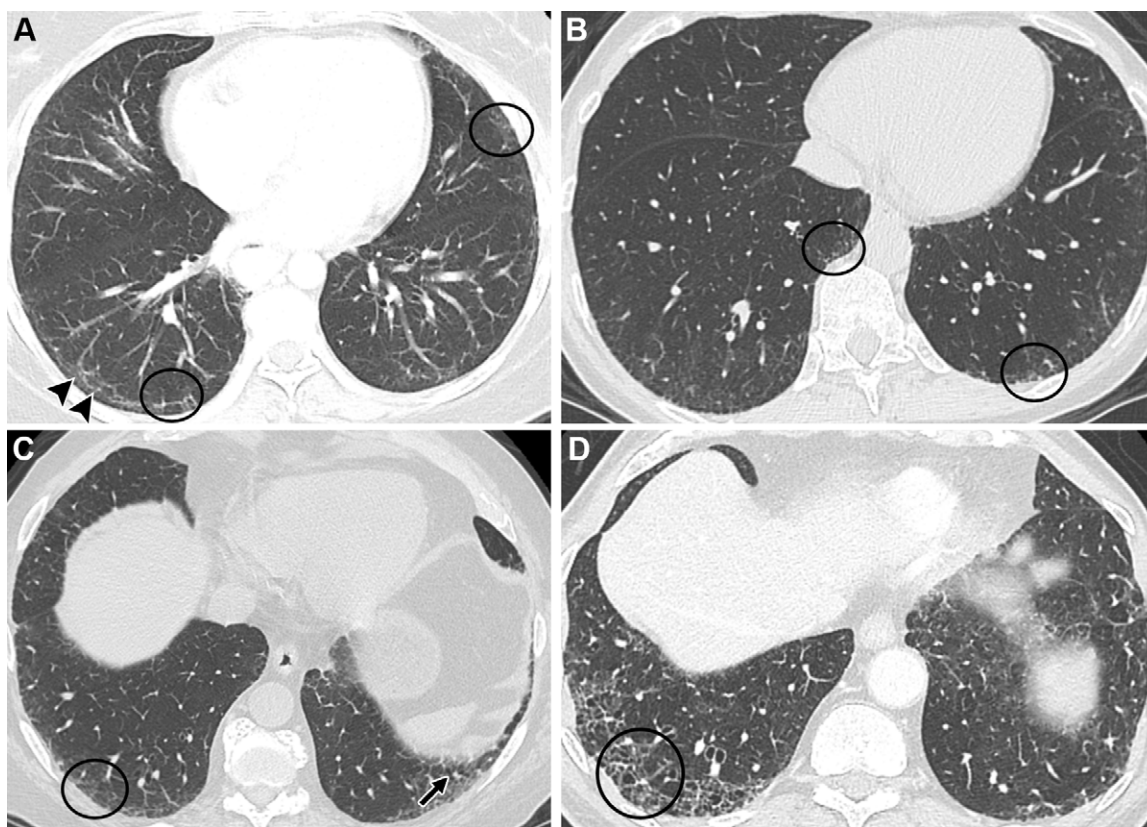


**Figure 11:** Images in four patients with interstitial lung abnormality (ILA). **(A)** Unenhanced axial CT image in a 42-year-old female presenting with pleuritic chest pain shows peripheral reticulation of the lower lobes and lingula (circles) with relative subpleural sparing (arrowheads), compatible with nonsubpleural ILA. **(B)** Unenhanced axial CT image in a 60-year-old female presenting with weight loss shows mild lower lobe predominant reticulation (circles) without traction bronchiectasis and/or bronchiolectasis or honeycombing, compatible with nonfibrotic subpleural ILA. **(C)** Unenhanced axial CT image in a 69-year-old male presenting for metastatic work-up of recently diagnosed head and neck cancer shows lower lobe–predominant reticulation (circle) with mild traction bronchiolectasis (arrow), compatible with a probable usual interstitial pneumonia (UIP) pattern of fibrotic subpleural ILA. **(D)** Unenhanced axial CT image in a 77-year-old male presenting for metastatic work-up of head and neck cancer shows lower lobe–predominant honeycombing superimposed on reticulation (circle), compatible with a UIP pattern of fibrotic subpleural ILA.

under-reported and result in downstream pulmonology referrals in only about one-third of patients (81).

The 2020 Fleischner Society white paper provides a general framework for the characterization and follow-up of ILAs, excluding individuals with high risk (individuals with familial ILD, occupational exposures, and connective tissue disease–associated ILD) from the initial definition (20). The distinction of ILA from ILD is reliant on clinical assessment. ILAs are specific nondependent CT abnormalities (GGO, reticulation, nonemphysematous cysts, honeycombing, traction bronchiectasis, and architectural distortion) involving more than 5% of any of the six lung zones. ILAs are categorized as subpleural fibrotic, subpleural nonfibrotic, and nonsubpleural (Fig 11). Honeycombing, traction bronchiectasis, and architectural distortion are markers of fibrotic ILA, which can be categorized in accordance with the current UIP-centric classification as typical for UIP, probable UIP, or indeterminate for UIP.

Adequate terminology is critical, as imaging aids in prognostication. High-risk imaging features, including reticulation and subpleural fibrotic forms of the typical or probable UIP subtypes, should be emphasized in radiology reports, as these impact follow-up and management considerations; ILAs characterized by honeycombing are invariably associated with progression (21,77,82). The identification of ILAs should trigger a

thorough clinical assessment to assess symptoms and pulmonary function and to exclude underlying risk factors for ILD. Assuming clinical stability, 1–2-year follow-up CT should be considered for subpleural ILAs, particularly when fibrotic (20,66).

### Quantitative ILD Imaging and the Promise of AI

Qualitative CT assessment of ILAs and ILD remains subject to substantial inter-reader variability and relatively low sensitivity to early or subtle changes at follow-up, even for experienced thoracic radiologists (83,84). Reliable characterization and stratification of patients at risk for progression remains challenging. Emerging AI tools bring great promise for greater reproducibility and reliability of ILAs and/or ILD identification, classification, prognostication, and follow-up. Quantitative tools explored in ILD most commonly rely on machine learning algorithms trained to recognize complex CT patterns and deep learning algorithms using convolutional neural networks for the automated extraction of CT patterns (85).

Computer-based tools can aid ILD diagnosis and classification. High attenuation areas, defined as the percentage of lung voxels between –600 and –250 HU at CT and reliant on automated threshold measurements, were shown to be associated with lung remodeling, inflammation biomarkers, ILAs, ILD-related hospitalization, and all-cause mortality in patients with ILD

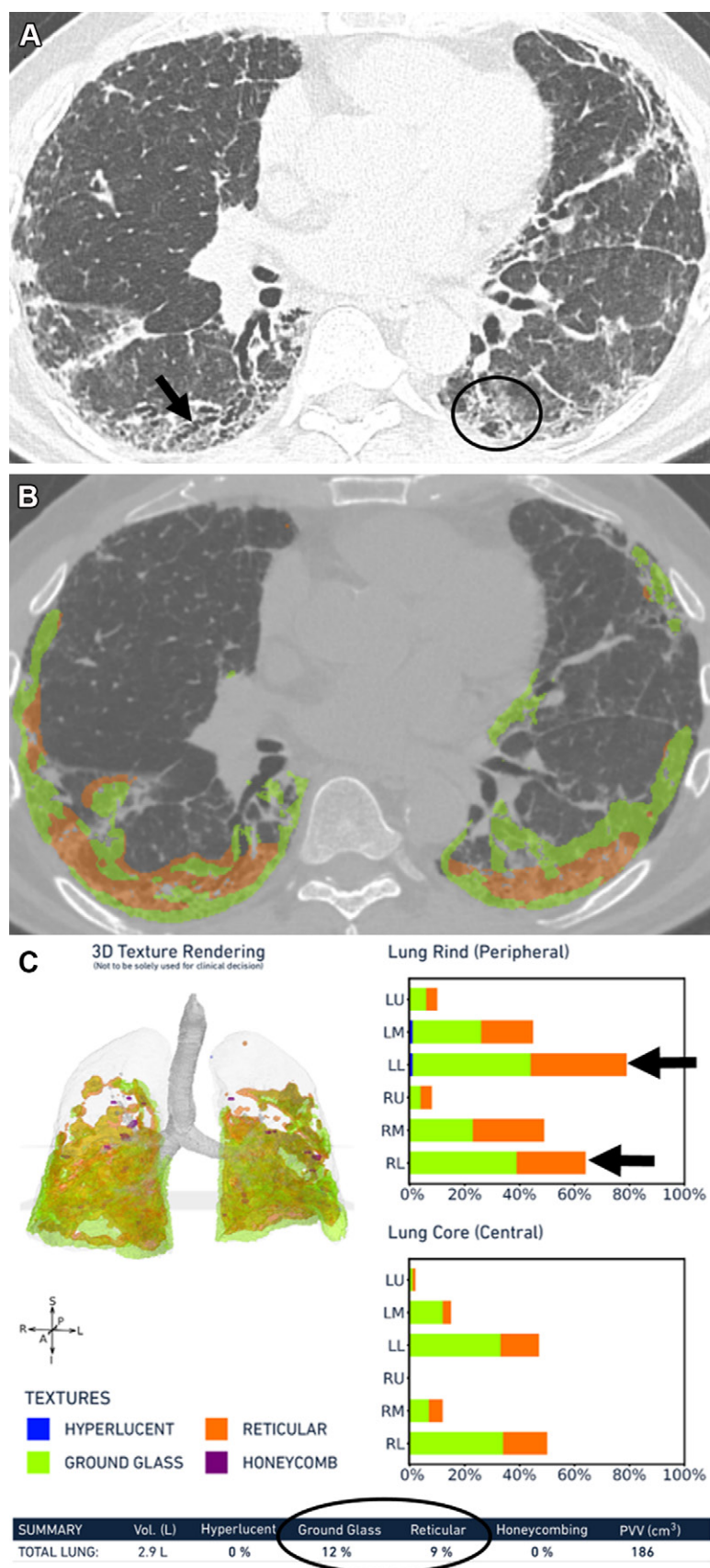


**Figure 12:** Images of lung texture analysis in a 69-year-old male with familial pulmonary fibrosis. **(A)** Unenhanced axial CT image in lung window demonstrates lower lobe- and peripheral-predominant fibrosis primarily characterized by ground-glass opacity (GGO) and reticulation (circle) and traction bronchiectasis (arrow). **(B)** Corresponding lung texture analysis overlay map and **(C)** lung texture analysis summary report highlight the distribution of abnormality, most pronounced in the peripheral lower lobes (arrows in **C**) and provide percentages of lung tissue involvement in each classification (circled area in **C**) (12% for GGO and 9% for reticulation). LL = left lower, LM = left middle, LU = left upper, PVV = pulmonary vascular volume, RL = right lower, RM = right middle, RU = right upper, 3D = three-dimensional.

UIP from non-UIP patterns (89–91). A recently described radiomic classifier demonstrated good performance in predicting radiologist-determined UIP (90). A machine learning model approved by the Food and Drug Administration for use in ILD showed high sensitivity in classifying IPF in patients with lower-confidence UIP imaging patterns (92). These algorithms are particularly interesting when subspecialized radiology expertise is lacking and when high-confidence diagnosis cannot be reached at qualitative CT assessment.

Lung texture analysis tools are CT-derived quantitative measures of lung fibrosis (Fig 12). Such methods have been explored as measures of disease severity and progression and as potential prognostic metrics, most extensively in IPF. These tools map fibrotic parenchyma by enabling detection and quantification of various lung textures, including high-attenuation areas, reticulation, and honeycombing. An example is the data-driven texture analysis fibrosis score, defined as the volume of fibrotic abnormality expressed as a percentage of the entire lung volume (88,93). Data-driven texture analysis scores correlate with disease severity, pulmonary function tests at baseline and follow-up, and mortality (94,95). A threshold data-driven texture analysis score change of approximately 3.5% was previously found to reflect clinically significant change (93). Changes in fibrosis scores in patients with HP and IPF also helped predict survival using another lung texture analysis tool (96,97). Increased pulmonary vessel volumes derived from lung texture analysis were associated with increased ILD mortality in several reports (97,98). Baseline quantitative ILD scores, defined as the sum of lung fibrosis extent, GGO, and honeycombing, were associated with disease severity and subsequent progression in idiopathic inflammatory myositis and with treatment response in scleroderma (88,99). These lung texture analysis-based quantitative scores can therefore serve as disease severity and progression markers and prognostic determinants in ILD.

Emerging AI models are therefore promising adjunct tools to qualitative CT assessment, although many remain experimental. To allow broader implementation of AI into clinical practice, validation against clinical and radiologic data are crucial, while addressing data sharing and privacy concerns (100).

(86,87). Although nonspecific, high-attenuation areas may help in the early detection of ILD and the prognostication of patients (88). Deep learning algorithms capable of autonomously classifying CT patterns showed good performance in distinguishing



## Summary and Practical Approach

Interstitial lung disease (ILD) diagnosis is continuously evolving and often challenging. Multidisciplinary discussion is the reference standard, aided by a thorough and systematic radiologic review. A critical first step at CT is distinguishing fibrotic from nonfibrotic subtypes. Fibrosis in ILD is a critical determinant of prognosis, particularly when features of usual interstitial pneumonia (UIP) are identified. In fibrotic ILDs, a UIP-centric imaging approach first guides the diagnosis by determining the level of confidence for UIP. Imaging clues help discern secondary UIP-like patterns from idiopathic pulmonary fibrosis. With non-UIP patterns, a thorough evaluation of predominant features and distribution are critical. Follow-up imaging aids the decision to initiate antifibrotics in progressive pulmonary fibrosis. In conclusion, CT is the cornerstone for ILD diagnosis, prognostication, and follow-up at multidisciplinary discussion. Radiologists play a critical role in the diagnosis of ILD and should familiarize themselves with evolving and novel ILD concepts.

**Deputy Editor:** Mizuki Nishino

**Scientific Editor:** Sarah Atzen

### Author affiliations:

<sup>1</sup> Department of Diagnostic Radiology, University of Chicago Medicine, Chicago, Ill

<sup>2</sup> Department of Radiology, Portland VA Healthcare System, Portland, Ore

<sup>3</sup> Department of Diagnostic Radiology, Section of Cardiothoracic Imaging, Oregon Health & Science University, Portland, Ore

<sup>4</sup> Department of Diagnostic Radiology, University of Kentucky, Lexington, Ky

<sup>5</sup> Department of Radiology, University of Wisconsin–Madison, Madison, Wis

<sup>6</sup> Department of Radiology, National Jewish Health, Denver, Colo

<sup>7</sup> Department of Radiology, University of California–San Diego, 9300 Campus Point Dr, San Diego, CA 92037

Received August 23, 2024; revision requested September 27; final revision received March 31, 2025; accepted April 14.

**Address correspondence to:** J.H.C. (email: Jherochung@health.ucsd.edu).

**Funding:** Authors declared no funding for this work.

**Disclosures of conflicts of interest:** L.C. Payment or honoraria for lectures, presentations, or educational events from Boehringer Ingelheim. A.G.B. No relevant relationships. S.B.H. No relevant relationships. J.P.K. No relevant relationships. S.J.K. Compensation from Boehringer Ingelheim for providing an hour lecture. D.A.L. Consulting fees from Calyx, Boehringer Ingelheim, Daiichi Sankyo, AstraZeneca; payment or honoraria for lectures, presentations, speakers bureaus, manuscript writing, or educational events from Clinical Education Alliance. J.H.C. Consulting fees from Boehringer Ingelheim; payment or honoraria for lectures, presentations, speakers bureaus, manuscript writing or educational events from Boehringer Ingelheim.

## References

- Ageely G, Souza C, De Boer K, Zahra S, Gomes M, Voduc N. The Impact of Multidisciplinary Discussion (MDD) in the Diagnosis and Management of Fibrotic Interstitial Lung Diseases. *Can Respir J* 2020;2020:9026171.
- Kaul B, Cottin V, Collard HR, Valenzuela C. Variability in Global Prevalence of Interstitial Lung Disease. *Front Med (Lausanne)* 2021;8:751181.
- Todo G, Ito H, Nakano Y, et al. [High resolution CT (HR-CT) for the evaluation of pulmonary peripheral disorders]. *Rinsho Hoshasen* 1982;27(12):1319–1326.
- Raghu G, Remy-Jardin M, Myers JL, et al; American Thoracic Society, European Respiratory Society, Japanese Respiratory Society, and Latin American Thoracic Society. An Official ATS/ERS/JRS/ALAT Clinical Practice Guideline. *Am J Respir Crit Care Med* 2018;198(5):e44–e68.
- Hobbs S, Chung JH, Leb J, Kaproth-Joslin K, Lynch DA. Practical Imaging Interpretation in Patients Suspected of Having Idiopathic Pulmonary Fibrosis: Official Recommendations from the Radiology Working Group of the Pulmonary Fibrosis Foundation. *Radiol Cardiothorac Imaging* 2021;3(1):e200279.
- Padole A, Ali Khawaja RD, Kalra MK, Singh S. CT radiation dose and iterative reconstruction techniques. *AJR Am J Roentgenol* 2015;204(4):W384–392.
- Mileto A, Guimaraes LS, McCollough CH, Fletcher JG, Yu L. State of the Art in Abdominal CT: The Limits of Iterative Reconstruction Algorithms. *Radiology* 2019;293(3):491–503.
- Wittram C, Mark EJ, McLoud TC. CT-histologic correlation of the ATS/ERS 2002 classification of idiopathic interstitial pneumonias. *Radiographics* 2003;23(5):1057–1071.
- Romei C, Tavanti L, Sbragia P, et al. Idiopathic interstitial pneumonias: do HRCT criteria established by ATS/ERS/JRS/ALAT in 2011 predict disease progression and prognosis? *Radiol Med* 2015;120(10):930–940.
- Travis WD, Costabel U, Hansell DM, et al; ATS/ERS Committee on Idiopathic Interstitial Pneumonias. An official American Thoracic Society/European Respiratory Society statement: Update of the international multidisciplinary classification of the idiopathic interstitial pneumonias. *Am J Respir Crit Care Med* 2013;188(6):733–748.
- Demedts M, Costabel U. ATS/ERS international multidisciplinary consensus classification of the idiopathic interstitial pneumonias. *Eur Respir J* 2002;19(5):794–796.
- Lee KS, Han J, Wada N, et al. Imaging of Pulmonary Fibrosis: An Update, From the *AJR* Special Series on Imaging of Fibrosis. *AJR Am J Roentgenol* 2024;222(2):e2329119.
- Raghu G, Remy-Jardin M, Richeldi L, et al. Idiopathic Pulmonary Fibrosis (an Update) and Progressive Pulmonary Fibrosis in Adults: An Official ATS/ERS/JRS/ALAT Clinical Practice Guideline. *Am J Respir Crit Care Med* 2022;205(9):e18–e47.
- Lynch DA, Sverzellati N, Travis WD, et al. Diagnostic criteria for idiopathic pulmonary fibrosis: a Fleischner Society White Paper. *Lancet Respir Med* 2018;6(2):138–153.
- Gruden JF, Green DB, Girvin FG, Naidich DP. Current Imaging of Idiopathic Pulmonary Fibrosis. *Radiol Clin North Am* 2022;60(6):873–888.
- Chung JH, Cox CW, Montner SM, et al. CT Features of the Usual Interstitial Pneumonia Pattern: Differentiating Connective Tissue Disease-Associated Interstitial Lung Disease From Idiopathic Pulmonary Fibrosis. *AJR Am J Roentgenol* 2018;210(2):307–313.
- Silva CIS, Müller NL, Hansell DM, Lee KS, Nicholson AG, Wells AU. Nonspecific interstitial pneumonia and idiopathic pulmonary fibrosis: changes in pattern and distribution of disease over time. *Radiology* 2008;247(1):251–259.
- Flaherty KR, Thwaite EL, Kazerooni EA, et al. Radiological versus histological diagnosis in UIP and NSIP: survival implications. *Thorax* 2003;58(2):143–148.
- Brownell R, Moua T, Henry TS, et al. The use of pretest probability increases the value of high-resolution CT in diagnosing usual interstitial pneumonia. *Thorax* 2017;72(5):424–429.
- Hatabu H, Hunninghake GM, Richeldi L, et al. Interstitial lung abnormalities detected incidentally on CT: a Position Paper from the Fleischner Society. *Lancet Respir Med* 2020;8(7):726–737.
- Araki T, Putman RK, Hatabu H, et al. Development and Progression of Interstitial Lung Abnormalities in the Framingham Heart Study. *Am J Respir Crit Care Med* 2016;194(12):1514–1522.
- Raghu G, Remy-Jardin M, Myers J, Richeldi L, Wilson KC. The 2018 Diagnosis of Idiopathic Pulmonary Fibrosis Guidelines: Surgical Lung Biopsy for Radiological Pattern of Probable Usual Interstitial Pneumonia Is Not Mandatory. *Am J Respir Crit Care Med* 2019;200(9):1089–1092.
- Maher TM, Strek ME. Antifibrotic therapy for idiopathic pulmonary fibrosis: time to treat. *Respir Res* 2019;20(1):205.
- Shah RM, Kolansky AM, Kligerman S. Thin-Section CT in the Categorization and Management of Pulmonary Fibrosis including Recently Defined Progressive Pulmonary Fibrosis. *Radiol Cardiothorac Imaging* 2024;6(1):e230135.
- Lynch DA, Godwin JD, Safrin S, et al; Idiopathic Pulmonary Fibrosis Study Group. High-resolution computed tomography in idiopathic pulmonary fibrosis: diagnosis and prognosis. *Am J Respir Crit Care Med* 2005;172(4):488–493.
- Adegunsoye A, Oldham JM, Bellam SK, et al. Computed Tomography Honeycombing Identifies a Progressive Fibrotic Phenotype with Increased Mortality across Diverse Interstitial Lung Diseases. *Ann Am Thorac Soc* 2019;16(5):580–588.
- Adams TN, Batra K, Kypreos M, Glazer CS. Impact of radiographic honeycombing on transplant free survival and efficacy of immunosuppression in fibrotic hypersensitivity pneumonitis. *BMC Pulm Med* 2023;23(1):224.
- Salisbury ML, Tolle LB, Xia M, et al. Possible UIP pattern on high-resolution computed tomography is associated with better survival than definite UIP in IPF patients. *Respir Med* 2017;131:229–235.



29. Fukihara J, Kondoh Y, Brown KK, et al. Probable usual interstitial pneumonia pattern on chest CT: is it sufficient for a diagnosis of idiopathic pulmonary fibrosis? *Eur Respir J* 2020;55(4):1802465.
30. Sumikawa H, Johkoh T, Colby TV, et al. Computed tomography findings in pathological usual interstitial pneumonia: relationship to survival. *Am J Respir Crit Care Med* 2008;177(4):433–439.
31. Mai C, Verleden SE, McDonough JE, et al. Thin-Section CT Features of Idiopathic Pulmonary Fibrosis Correlated with Micro-CT and Histologic Analysis. *Radiology* 2017;283(1):252–263.
32. Galvin JR, Frazier AA, Franks TJ. Collaborative radiologic and histopathologic assessment of fibrotic lung disease. *Radiology* 2010;255(3):692–706.
33. Maher TM. Interstitial Lung Disease: A Review. *JAMA* 2024;331(19):1655–1665.
34. Raghu G, Remy-Jardin M, Ryerson CJ, et al. Diagnosis of Hypersensitivity Pneumonitis in Adults. An Official ATS/JRS/ALAT Clinical Practice Guideline. *Am J Respir Crit Care Med* 2020;202(3):e36–e69.
35. Kim EA, Lee KS, Johkoh T, et al. Interstitial lung diseases associated with collagen vascular diseases: radiologic and histopathologic findings. *RadioGraphics* 2002;22 Spec No:S151–S165.
36. Akira M, Morinaga K. The comparison of high-resolution computed tomography findings in asbestosis and idiopathic pulmonary fibrosis. *Am J Ind Med* 2016;59(4):301–306.
37. Matyga AW, Chelala L, Chung JH. Occupational Lung Diseases: Spectrum of Common Imaging Manifestations. *Korean J Radiol* 2023;24(8):795–806.
38. American Thoracic Society. Diagnosis and initial management of nonmalignant diseases related to asbestos. *Am J Respir Crit Care Med* 2004;170(6):691–715.
39. Brady D, Berkowitz EA, Sharma A, et al. CT Morphologic Characteristics and Variant Patterns of Interstitial Pulmonary Fibrosis in Systemic Lupus Erythematosus. *Radiol Cardiothorac Imaging* 2021;3(4):e200625.
40. White CS. Interstitial Pulmonary Fibrosis in Systemic Lupus Erythematosus: Are There Variants of the Variant Fibrotic Patterns? *Radiol Cardiothorac Imaging* 2021;3(4):e210183.
41. Chung JH, Montner SM, Thirkath P, Cannon B, Barnett SD, Nathan SD. Computed Tomography Findings Suggestive of Connective Tissue Disease in the Setting of Usual Interstitial Pneumonia. *J Comput Assist Tomogr* 2021;45(5):776–781.
42. Walkoff L, White DB, Chung JH, Asante D, Cox CW. The Four Corners Sign: A Specific Imaging Feature in Differentiating Systemic Sclerosis-related Interstitial Lung Disease From Idiopathic Pulmonary Fibrosis. *J Thorac Imaging* 2018;33(3):197–203.
43. Yoo H, Hino T, Hwang J, et al. Connective tissue disease-related interstitial lung disease (CTD-ILD) and interstitial lung abnormality (ILA): Evolving concept of CT findings, pathology and management. *Eur J Radiol Open* 2022;9:100419.
44. Chelala L, Adegunsoye A, Cody BA, Husain AN, Chung JH. Updated Imaging Classification of Hypersensitivity Pneumonitis. *Radiol Clin North Am* 2022;60(6):901–913.
45. Hanak V, Golbin JM, Hartman TE, Ryu JH. High-resolution CT findings of parenchymal fibrosis correlate with prognosis in hypersensitivity pneumonitis. *Chest* 2008;134(1):133–138.
46. Mooney JJ, Elicker BM, Urbani TH, et al. Radiographic fibrosis score predicts survival in hypersensitivity pneumonitis. *Chest* 2013;144(2):586–592.
47. Fernández Pérez ER, Travis WD, Lynch DA, et al. Diagnosis and Evaluation of Hypersensitivity Pneumonitis: CHEST Guideline and Expert Panel Report. *Chest* 2021;160(2):e97–e156.
48. Hamblin M, Prosch H, Vašáková M. Diagnosis, course and management of hypersensitivity pneumonitis. *Eur Respir Rev* 2022;31(163):210169.
49. Chelala L, Adegunsoye A, Strek M, et al. Hypersensitivity Pneumonitis on Thin-Section Chest CT Scans: Diagnostic Performance of the ATS/JRS/ALAT versus ACCP Imaging Guidelines. *Radiol Cardiothorac Imaging* 2024;6(4):e230068.
50. Barnett J, Molyneux PL, Rawal B, et al. Variable utility of mosaic attenuation to distinguish fibrotic hypersensitivity pneumonitis from idiopathic pulmonary fibrosis. *Eur Respir J* 2019;54(1):1900531.
51. Kligerman SJ, Henry T, Lin CT, Franks TJ, Galvin JR. Mosaic Attenuation: Etiology, Methods of Differentiation, and Pitfalls. *RadioGraphics* 2015;35(5):1360–1380.
52. Marinescu DC, Raghu G, Remy-Jardin M, et al. Integration and Application of Clinical Practice Guidelines for the Diagnosis of Idiopathic Pulmonary Fibrosis and Fibrotic Hypersensitivity Pneumonitis. *Chest* 2022;162(3):614–629.
53. Lacasse Y, Cormier Y. Hypersensitivity pneumonitis. *Orphanet J Rare Dis* 2006;1:25.
54. Lynch DA, Rose CS, Way D, King TE Jr. Hypersensitivity pneumonitis: sensitivity of high-resolution CT in a population-based study. *AJR Am J Roentgenol* 1992;159(3):469–472.
55. Cottin V, Selman M, Inoue Y, et al. Syndrome of Combined Pulmonary Fibrosis and Emphysema: An Official ATS/ERS/JRS/ALAT Research Statement. *Am J Respir Crit Care Med* 2022;206(4):e7–e41.
56. Sato S, Tanino Y, Misa K, et al. Identification of Clinical Phenotypes in Idiopathic Interstitial Pneumonia with Pulmonary Emphysema. *Intern Med* 2016;55(12):1529–1535.
57. Mejía M, Carrillo G, Rojas-Serrano J, et al. Idiopathic pulmonary fibrosis and emphysema: decreased survival associated with severe pulmonary arterial hypertension. *Chest* 2009;136(1):10–15.
58. Cottin V. The impact of emphysema in pulmonary fibrosis. *Eur Respir Rev* 2013;22(128):153–157.
59. Papaioannou AI, Kostikas K, Manali ED, et al. Combined pulmonary fibrosis and emphysema: The many aspects of a cohabitation contract. *Respir Med* 2016;117:14–26.
60. Fleming H, Clifford SM, Haughey A, et al. Differentiating combined pulmonary fibrosis and emphysema from pure emphysema: utility of late gadolinium-enhanced MRI. *Eur Radiol Exp* 2020;4(1):61.
61. Chilosi M, Poletti V, Rossi A. The pathogenesis of COPD and IPF: distinct horns of the same devil? *Respir Res* 2012;13(1):3.
62. Yoon HY, Kim H, Bae Y, Song JW. Smoking status and clinical outcome in idiopathic pulmonary fibrosis: a nationwide study. *Respir Res* 2024;25(1):191.
63. Katzenstein ALA. Smoking-related interstitial fibrosis (SRIF), pathogenesis and treatment of usual interstitial pneumonia (UIP), and transbronchial biopsy in UIP. *Mod Pathol* 2012;25 Suppl 1:S68–S78.
64. Sousa C, Rodrigues M, Carvalho A, et al. Diffuse smoking-related lung diseases: insights from a radiologic-pathologic correlation. *Insights Imaging* 2019;10(1):73.
65. Rajan SK, Cottin V, Dhar R, et al. Progressive pulmonary fibrosis: an expert group consensus statement. *Eur Respir J* 2023;61(3):2103187.
66. Kanne JP, Walker CM, Brixey AG, et al. Progressive Pulmonary Fibrosis and Interstitial Lung Abnormalities: AJR Expert Panel Narrative Review. *AJR Am J Roentgenol* 2025;224(3):e2431125.
67. Shumar JN, Chandel A, King CS. Antifibrotic Therapies and Progressive Fibrosing Interstitial Lung Disease (PF-ILD): Building on INBUILD. *J Clin Med* 2021;10(11):2285.
68. Distler O, Highland KB, Gahlemann M, et al; SENSICIS Trial Investigators. Nintedanib for Systemic Sclerosis-Associated Interstitial Lung Disease. *N Engl J Med* 2019;380(26):2518–2528.
69. Flaherty KR, Wells AU, Cottin V, et al; INBUILD Trial Investigators. Nintedanib in Progressive Fibrosing Interstitial Lung Diseases. *N Engl J Med* 2019;381(18):1718–1727.
70. Hansell DM, Goldin JG, King TE, Lynch DA, Richeldi L, Wells AU. CT staging and monitoring of fibrotic interstitial lung diseases in clinical practice and treatment trials: a position paper from the Fleischner Society. *Lancet Respir Med* 2015;3(6):483–496.
71. Walsh SLE, Devaraj A, Enghelmayer JJ, et al. Role of imaging in progressive-fibrosing interstitial lung diseases. *Eur Respir Rev* 2018;27(150):180073.
72. Chung JH, Walker CM, Hobbs S. Imaging Features of Systemic Sclerosis-Associated Interstitial Lung Disease. *J Vis Exp* 2020;(160).
73. Washko GR, Hunninghake GM, Fernandez IE, et al; COPDGene Investigators. Lung volumes and emphysema in smokers with interstitial lung abnormalities. *N Engl J Med* 2011;364(10):897–906.
74. Flaherty KR, Wells AU, Cottin V, et al; INBUILD Trial Investigators. Nintedanib in progressive interstitial lung diseases: data from the whole INBUILD trial. *Eur Respir J* 2022;59(3):2004538.
75. Wells AU, Flaherty KR, Brown KK, et al; INBUILD trial investigators. Nintedanib in patients with progressive fibrosing interstitial lung diseases-subgroup analyses by interstitial lung disease diagnosis in the INBUILD trial: a randomised, double-blind, placebo-controlled, parallel-group trial. *Lancet Respir Med* 2020;8(5):453–460.
76. Hata A, Schiebler ML, Lynch DA, Hatabu H. Interstitial Lung Abnormalities: State of the Art. *Radiology* 2021;301(1):19–34.
77. Putman RK, Gudmundsson G, Axelsson GT, et al. Imaging Patterns Are Associated with Interstitial Lung Abnormality Progression and Mortality. *Am J Respir Crit Care Med* 2019;200(2):175–183.
78. Seok J, Park S, Yoon EC, Yoon HY. Clinical outcomes of interstitial lung abnormalities: a systematic review and meta-analysis. *Sci Rep* 2024;14(1):7330.
79. Whittaker Brown SA, Padilla M, Mhango G, et al. Interstitial Lung Abnormalities and Lung Cancer Risk in the National Lung Screening Trial. *Chest* 2019;156(6):1195–1203.
80. Putman RK, Hatabu H, Araki T, et al; COPDGene Investigators. Association Between Interstitial Lung Abnormalities and All-Cause Mortality. *JAMA* 2016;315(7):672–681.
81. Oldham JM, Adegunsoye A, Khera S, et al. Underreporting of Interstitial Lung Abnormalities on Lung Cancer Screening Computed Tomography. *Ann Am Thorac Soc* 2018;15(6):764–766.

82. Hunninghake GM, Goldin JG, Kadoch MA, et al; ILA Study Group. Detection and Early Referral of Patients With Interstitial Lung Abnormalities: An Expert Survey Initiative. *Chest* 2022;161(2):470–482.
83. Widell J, Lidén M. Interobserver variability in high-resolution CT of the lungs. *Eur J Radiol Open* 2020;7:100228.
84. Walsh SLF, Wells AU, Desai SR, et al. Multicentre evaluation of multidisciplinary team meeting agreement on diagnosis in diffuse parenchymal lung disease: a case-cohort study. *Lancet Respir Med* 2016;4(7):557–565.
85. Barnes H, Humphries SM, George PM, et al. Machine learning in radiology: the new frontier in interstitial lung diseases. *Lancet Digit Health* 2023;5(1):e41–e50.
86. Lederer DJ, Enright PL, Kawut SM, et al. Cigarette smoking is associated with subclinical parenchymal lung disease: the Multi-Ethnic Study of Atherosclerosis (MESA)-lung study. *Am J Respir Crit Care Med* 2009;180(5):407–414.
87. Choi B, Kawut SM, Raghu G, et al. Regional distribution of high-attenuation areas on chest computed tomography in the Multi-Ethnic Study of Atherosclerosis. *ERJ Open Res* 2020;6(1):00115–2019.
88. Chen A, Karwoski RA, Gierada DS, Bartholmai BJ, Koo CW. Quantitative CT Analysis of Diffuse Lung Disease. *RadioGraphics* 2020;40(1):28–43.
89. Park SO, Seo JB, Kim N, Lee YK, Lee J, Kim DS. Comparison of usual interstitial pneumonia and nonspecific interstitial pneumonia: quantification of disease severity and discrimination between two diseases on HRCT using a texture-based automated system. *Korean J Radiol* 2011;12(3):297–307.
90. Chung JH, Chelala L, Pugashetti JV, et al. A Deep Learning-Based Radiomic Classifier for Usual Interstitial Pneumonia. *Chest* 2024;165(2):371–380.
91. Walsh SLF, Calandriello L, Silva M, Sverzellati N. Deep learning for classifying fibrotic lung disease on high-resolution computed tomography: a case-cohort study. *Lancet Respir Med* 2018;6(11):837–845.
92. Bradley J, Huang J, Kalra A, Reicher J. External validation of Fibresolve, a machine-learning algorithm, to non-invasively diagnose idiopathic pulmonary fibrosis. *Am J Med Sci* 2024;367(3):195–200.
93. Humphries SM, Swigris JJ, Brown KK, et al. Quantitative high-resolution computed tomography fibrosis score: performance characteristics in idiopathic pulmonary fibrosis. *Eur Respir J* 2018;52(3):1801384.
94. Humphries SM, Yagihashi K, Huckleberry J, et al. Idiopathic Pulmonary Fibrosis: Data-driven Textural Analysis of Extent of Fibrosis at Baseline and 15-Month Follow-up. *Radiology* 2017;285(1):270–278.
95. Wells AU, Desai SR, Rubens MB, et al. Idiopathic pulmonary fibrosis: a composite physiologic index derived from disease extent observed by computed tomography. *Am J Respir Crit Care Med* 2003;167(7):962–969.
96. Maldonado F, Moua T, Rajagopalan S, et al. Automated quantification of radiological patterns predicts survival in idiopathic pulmonary fibrosis. *Eur Respir J* 2014;43(1):204–212.
97. Jacob J, Bartholmai BJ, Egashira R, et al. Chronic hypersensitivity pneumonitis: identification of key prognostic determinants using automated CT analysis. *BMC Pulm Med* 2017;17(1):81.
98. Jacob J, Bartholmai BJ, Rajagopalan S, et al. Mortality prediction in idiopathic pulmonary fibrosis: evaluation of computer-based CT analysis with conventional severity measures. *Eur Respir J* 2017;49(1):1601011.
99. Goldin JG, Kim GHJ, Tseng CH, et al. Longitudinal Changes in Quantitative Interstitial Lung Disease on Computed Tomography after Immunosuppression in the Scleroderma Lung Study II. *Ann Am Thorac Soc* 2018;15(11):1286–1295.
100. Felder FN, Walsh SLF. Exploring computer-based imaging analysis in interstitial lung disease: opportunities and challenges. *ERJ Open Res* 2023;9(4):00145–2023.